Climate System II

Glacial Climate, Orbital Theory

1. November 2022 (3rd lecture)

Gerrit Lohmann

Paleoclimate dynamics

- to identify driving mechanisms for climate change
- external forcing and internal variability of the climate system
- to test models of the Earth system

- statistical analysis of instrumental and proxy data.

Proxy Data

- Indirect data, often qualitative
- Long time series from archives
- Information beyond the instrumental record

Earth System: a polar perspective

Ice drilling camp, 2009

Polarstern, marine sediments

Lake/permafrost sediments

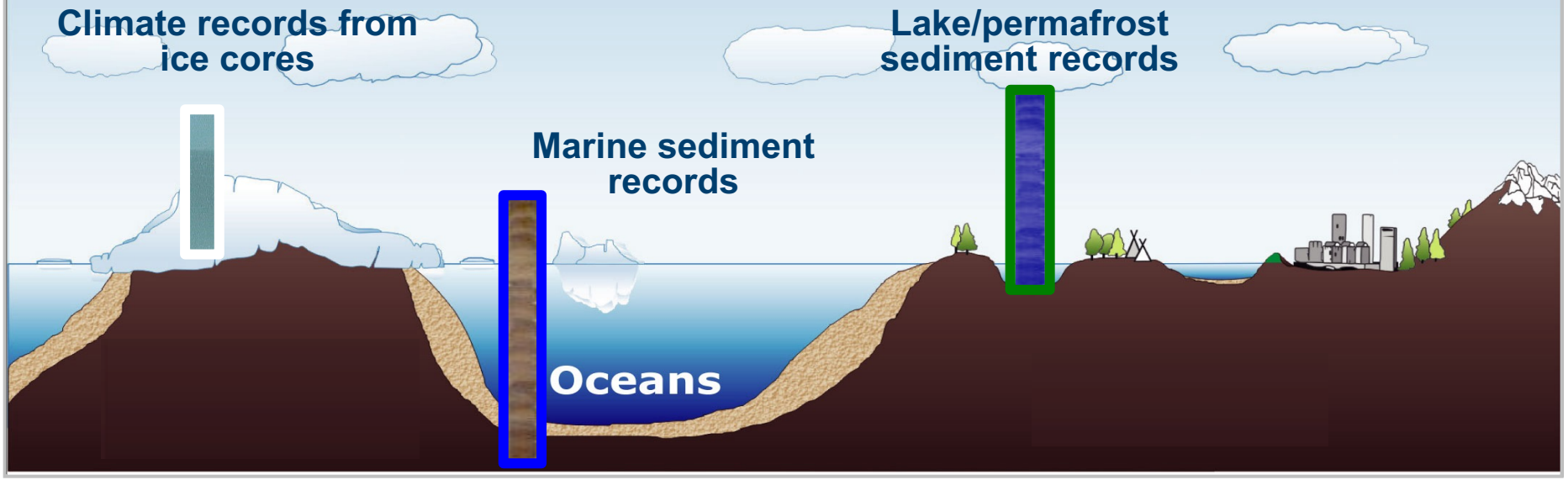

Climate Trends at different Timescales

Deglaciation – Greenland ice core

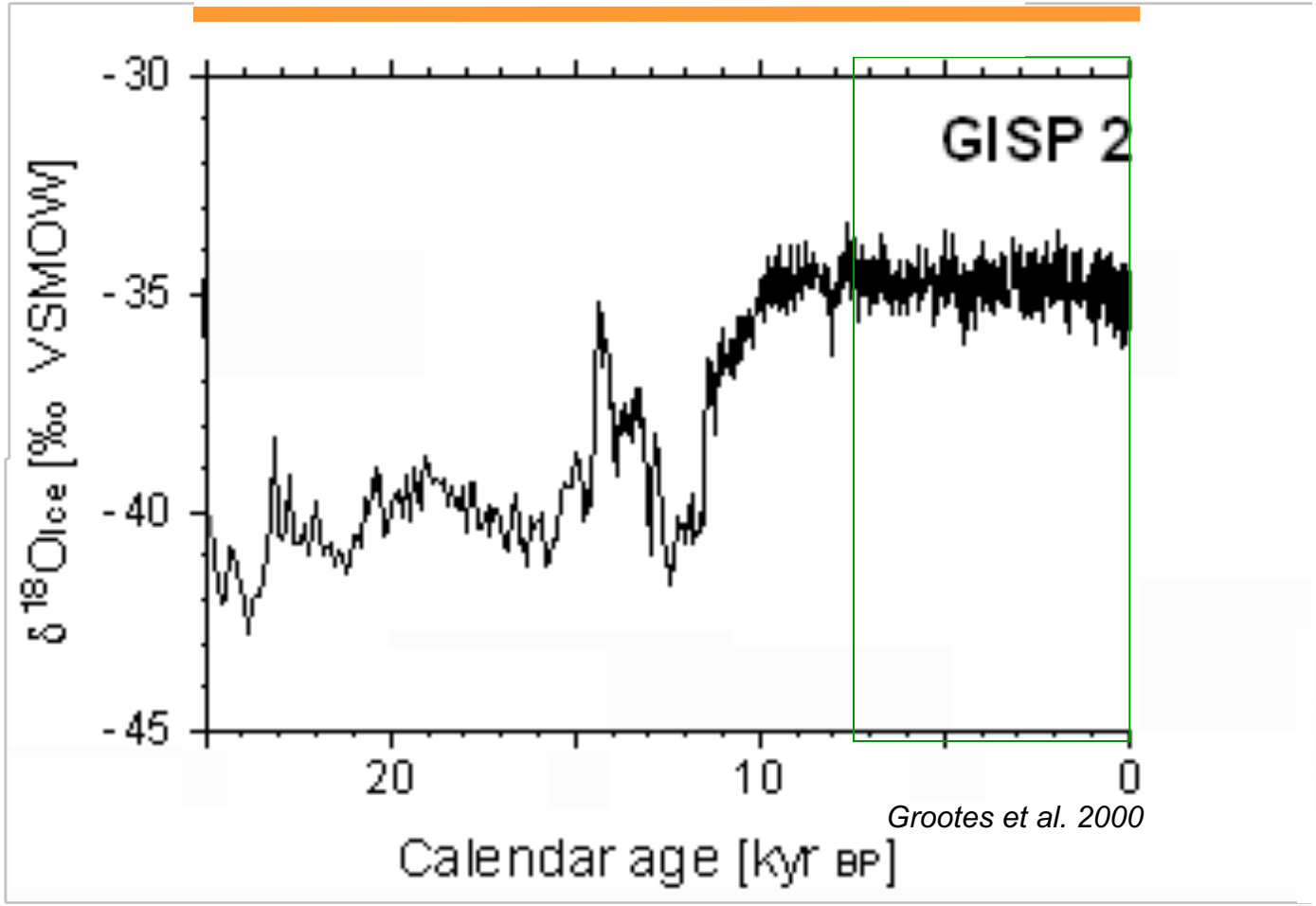

Grootes et al. 2000

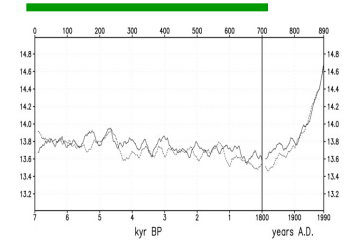

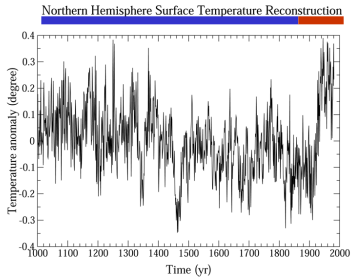

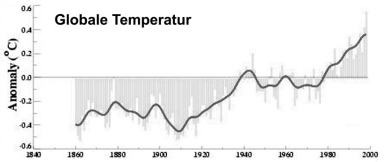

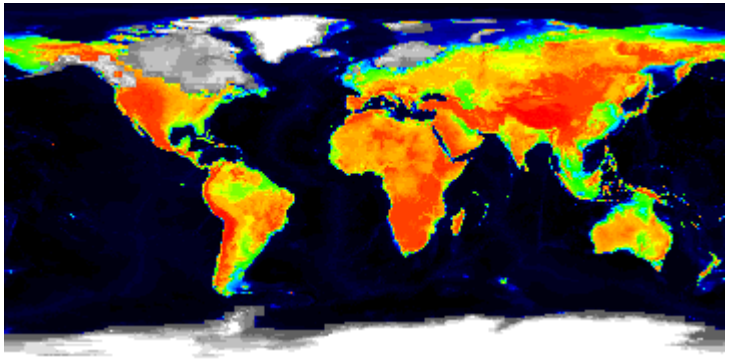

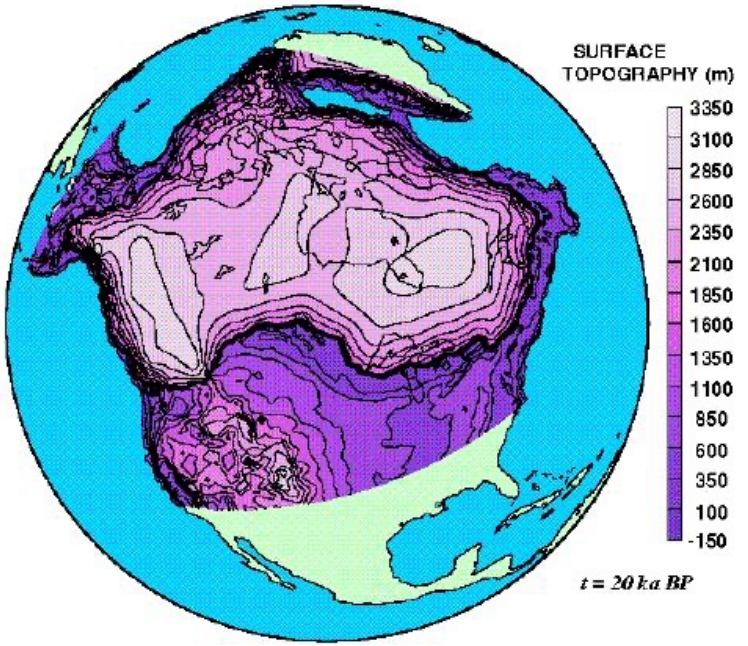

Deglaciation

The Brexit is not new !

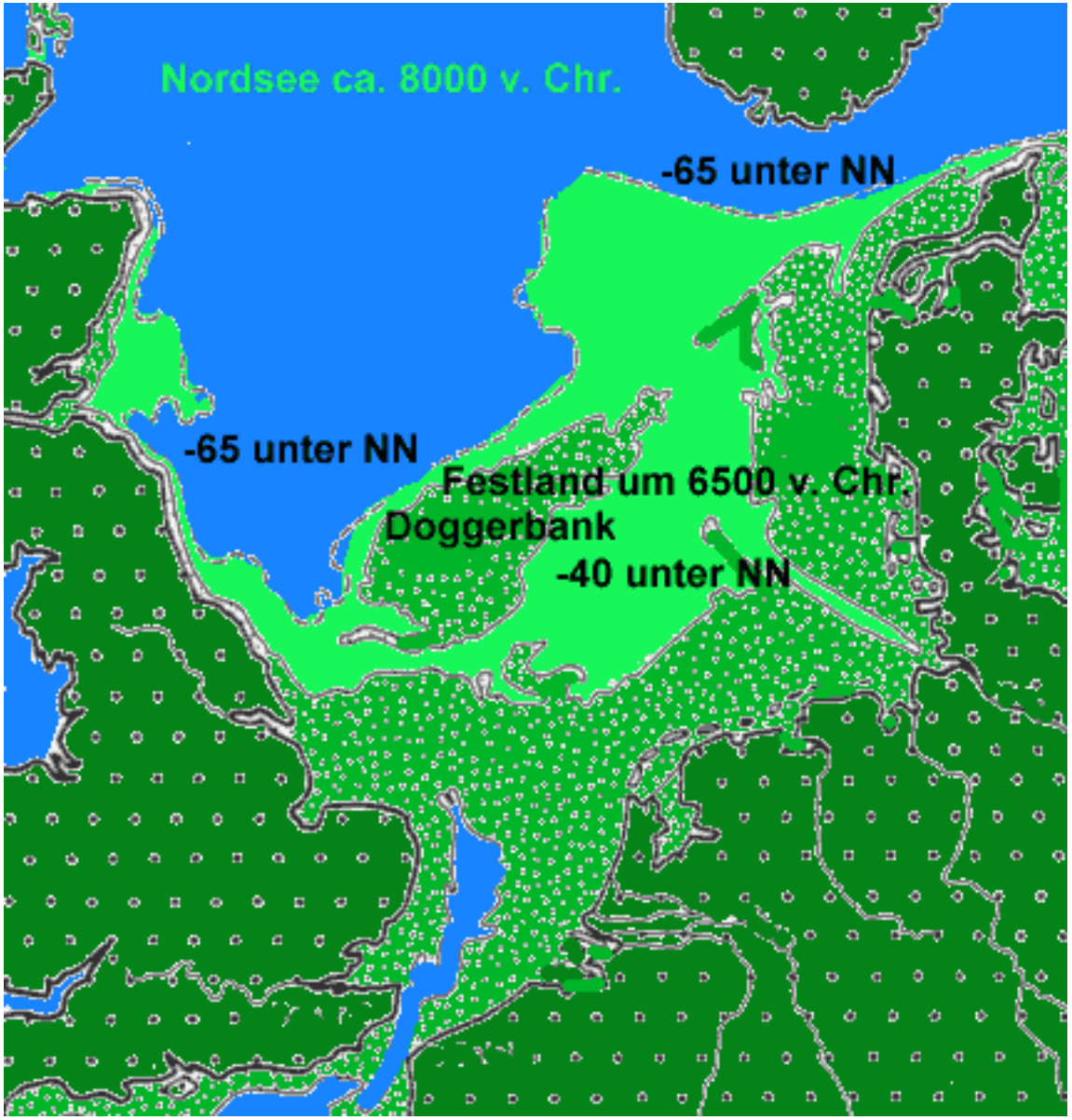

LGM climate of North America and Europe

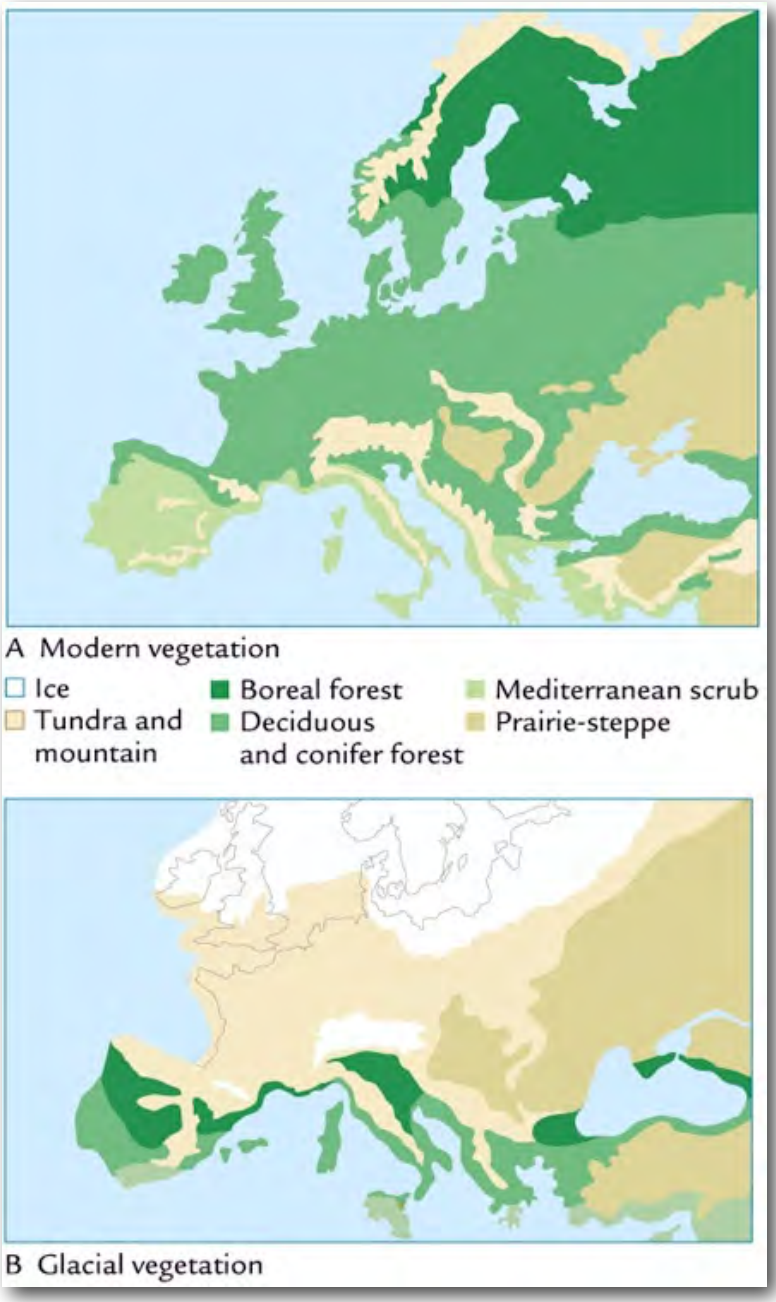

[from: Ruddiman, 2008]

Modern land cover

Glacial land cover

Atmospheric Gas Concentrations from Ice Cores

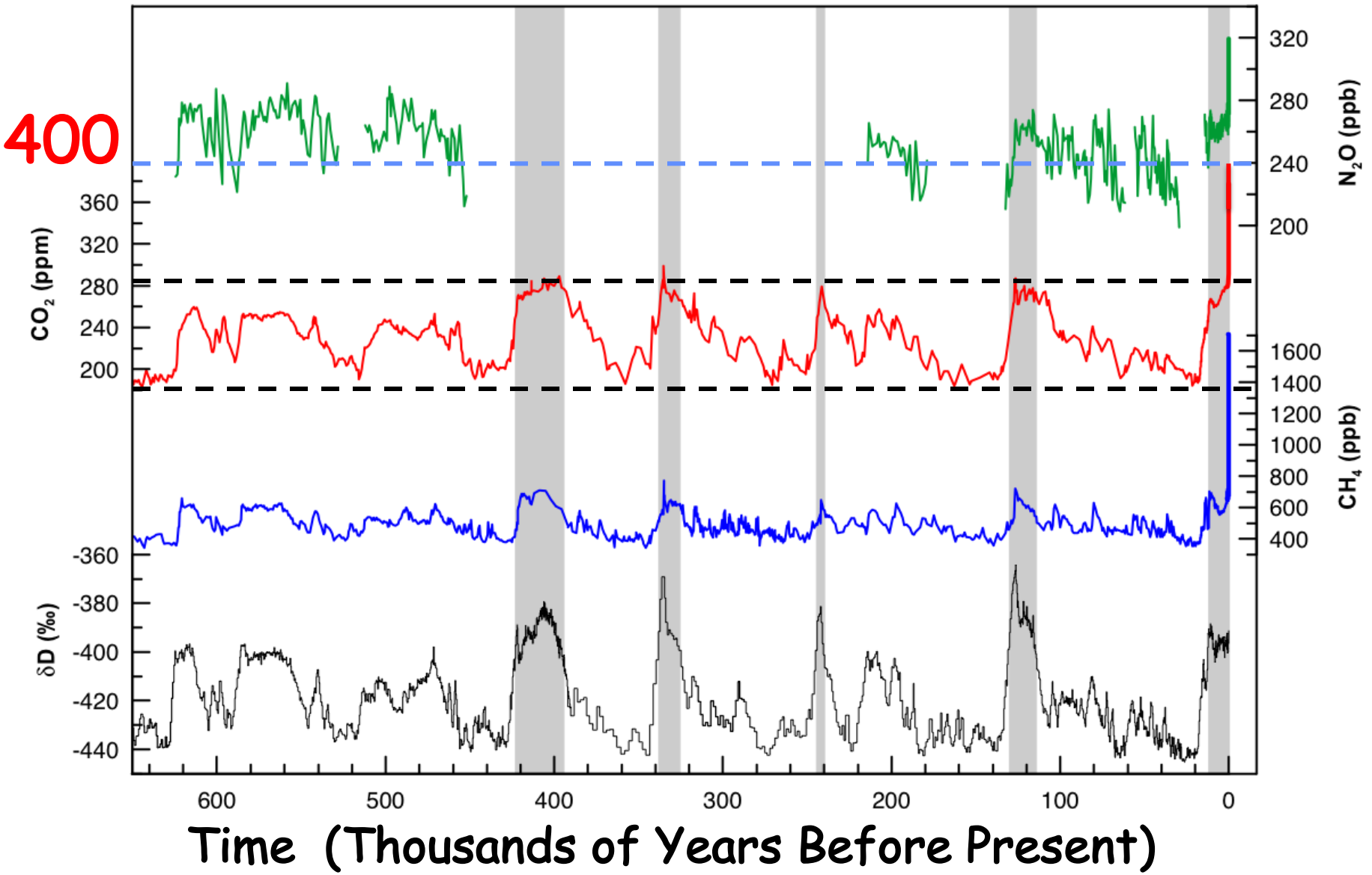

EPICA 2008

The Earth‘s orbit (shown with an exaggerated eccentricity ε)

$$r = \frac{a(1-\epsilon^2)}{1+\epsilon\cos\theta}$$

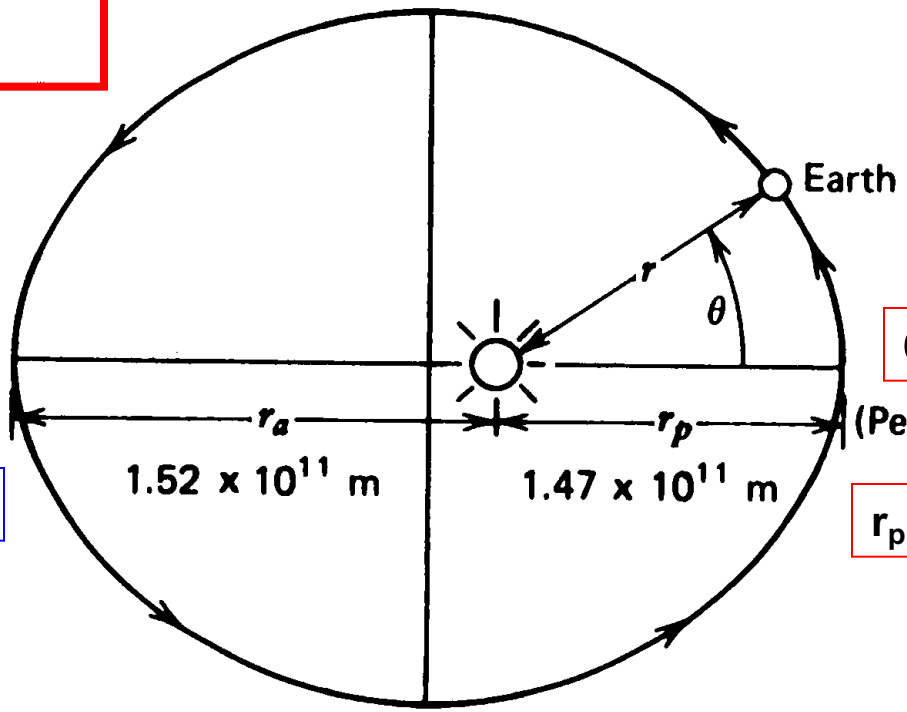

cos θ = -1

(Aphelion ~ July 4)

$r_a = r_{Aphelion} = a\,(1+\varepsilon)$

θ =0 ; cos θ =+ 1

(Perihelion ~ Jan. 4)

$r_p = r_{Perihelion} = a\,(1-\varepsilon)$

the mean orbital distance is **a = 149,7 [Gm]** = 149,7 Mio km
and the eccentricity is **ε = 0.0167**

Radius: r = a +/- 2%

Quelle: Wieder 1982

The tilt of
the Earth‘s axis

with respect to
its orbital plane
(ecliptic)

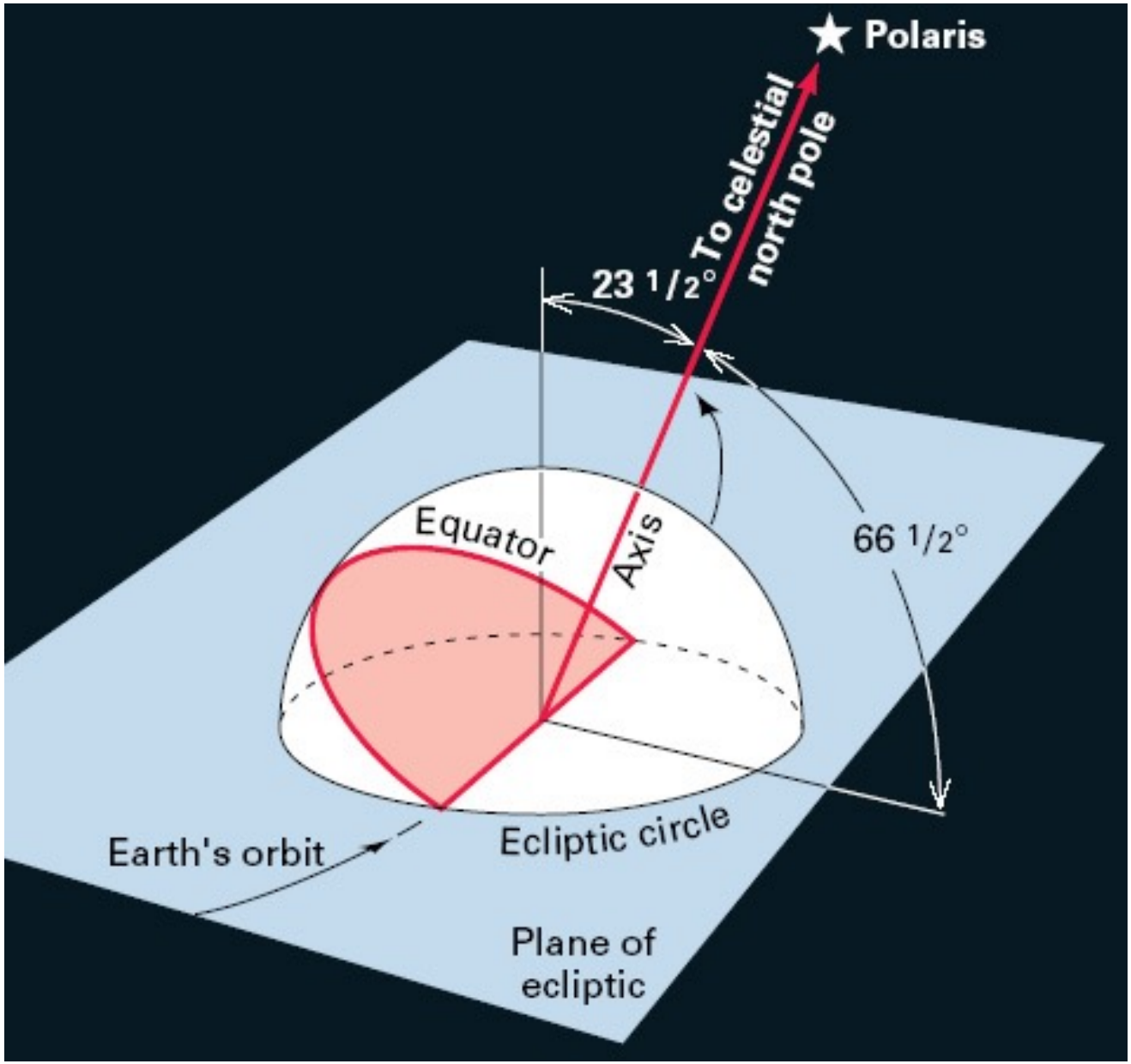

Strahler: „Physical Geography“,2002, Wiley

Seasons are a consequence of the inclination of the earth 's axis of rotation

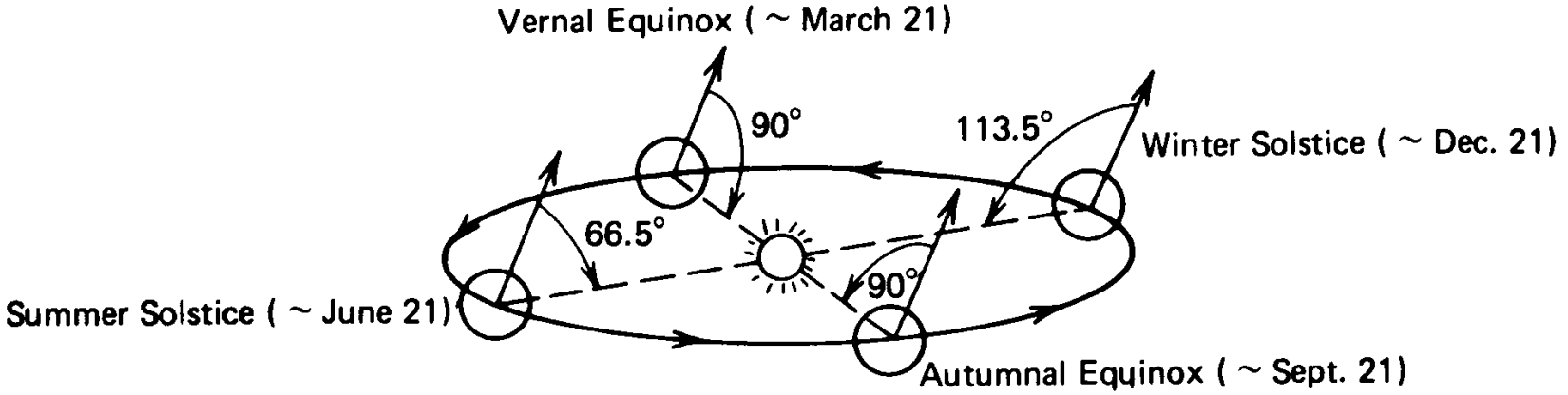

The **seasonal variation of the angle** between **the earth 's polar axis** and the **earth-sun line**.

The angle of inclination (between the **earth axis** of rotation and the **line perpendicular** to the **ecliptic** plane)
is 23.5˚ and remains constant throughout the year.

The rate of rotation is also constant and equal to one rotation every 23.93 hr = a sideral day..

Summer solstice (June 21) :	earth axis of rotation is tilted	90 - 23,5	= 66.5 ˚	toward the sun
Winter solstice (December 21) :		90 + 23.5	= 113.5˚	away from the sun
Autumnal equinox (September 23) :			90 ˚	
Vernal equinox (March 21) :			90˚	

Wieder 1982

The 4 seasons

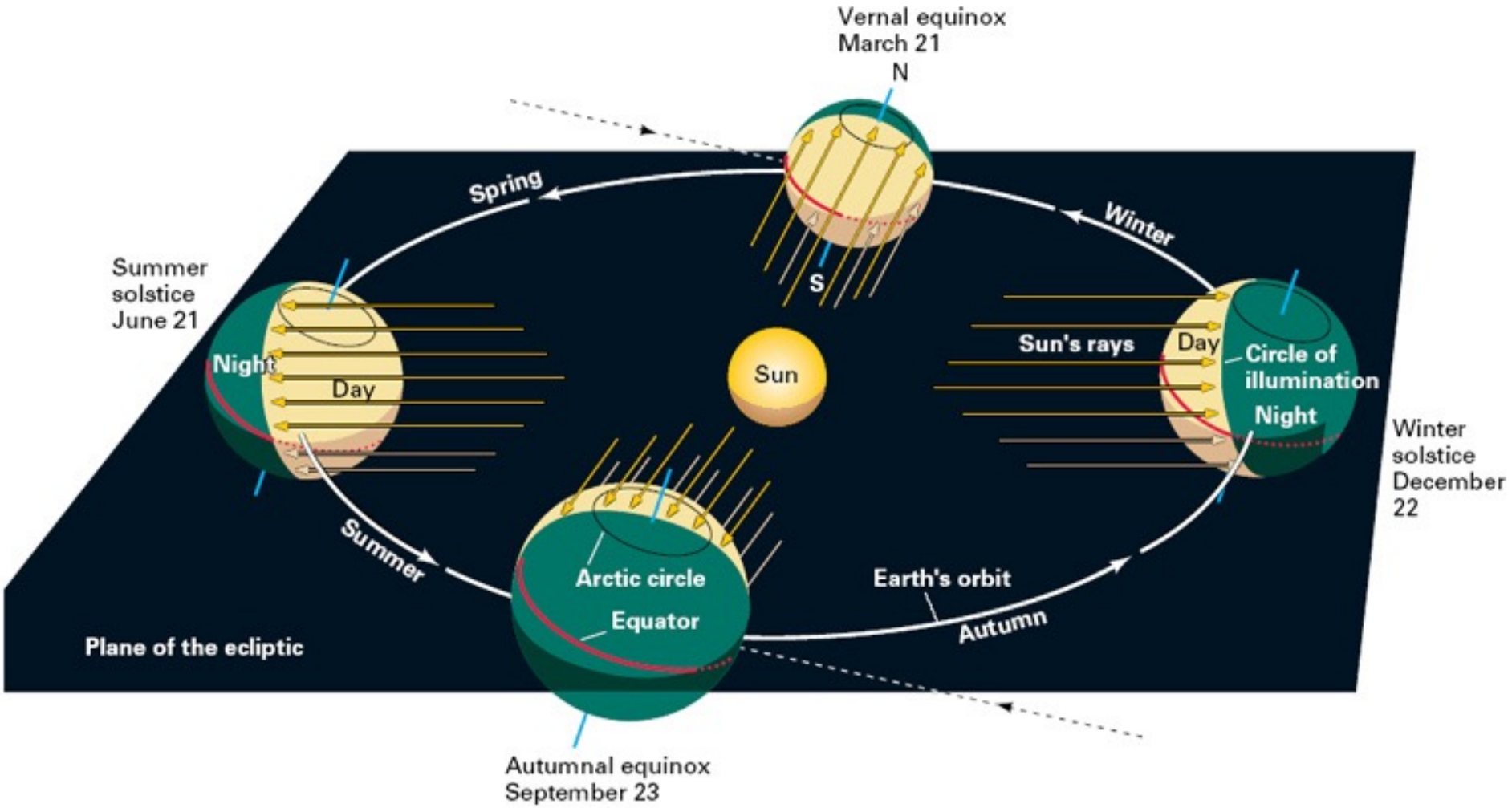

Strahler,2002

Equinox

at equinox, the circle of illumination passes through both poles

the subsolar point is the equator

each location on Earth experiences 12 hours of sunlight and 12 hours of darkness

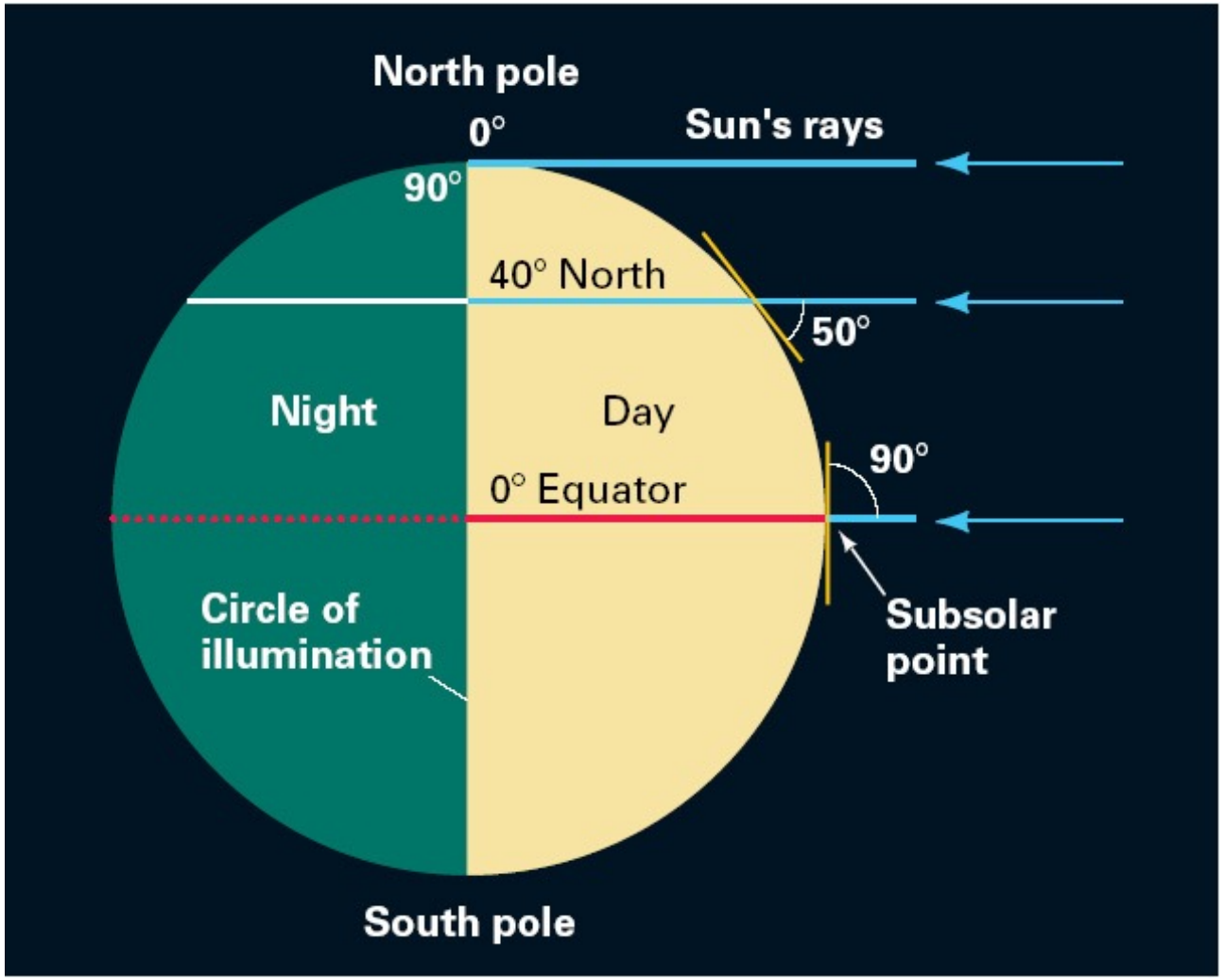

Strahler,2002

Solstice

Solstice (“sun stands still”)
On June 22, the subsolar point is 23½° N (Tropic of Cancer)
On Dec. 22, the subsolar point is 23½° S (Tropic of Capricorn)

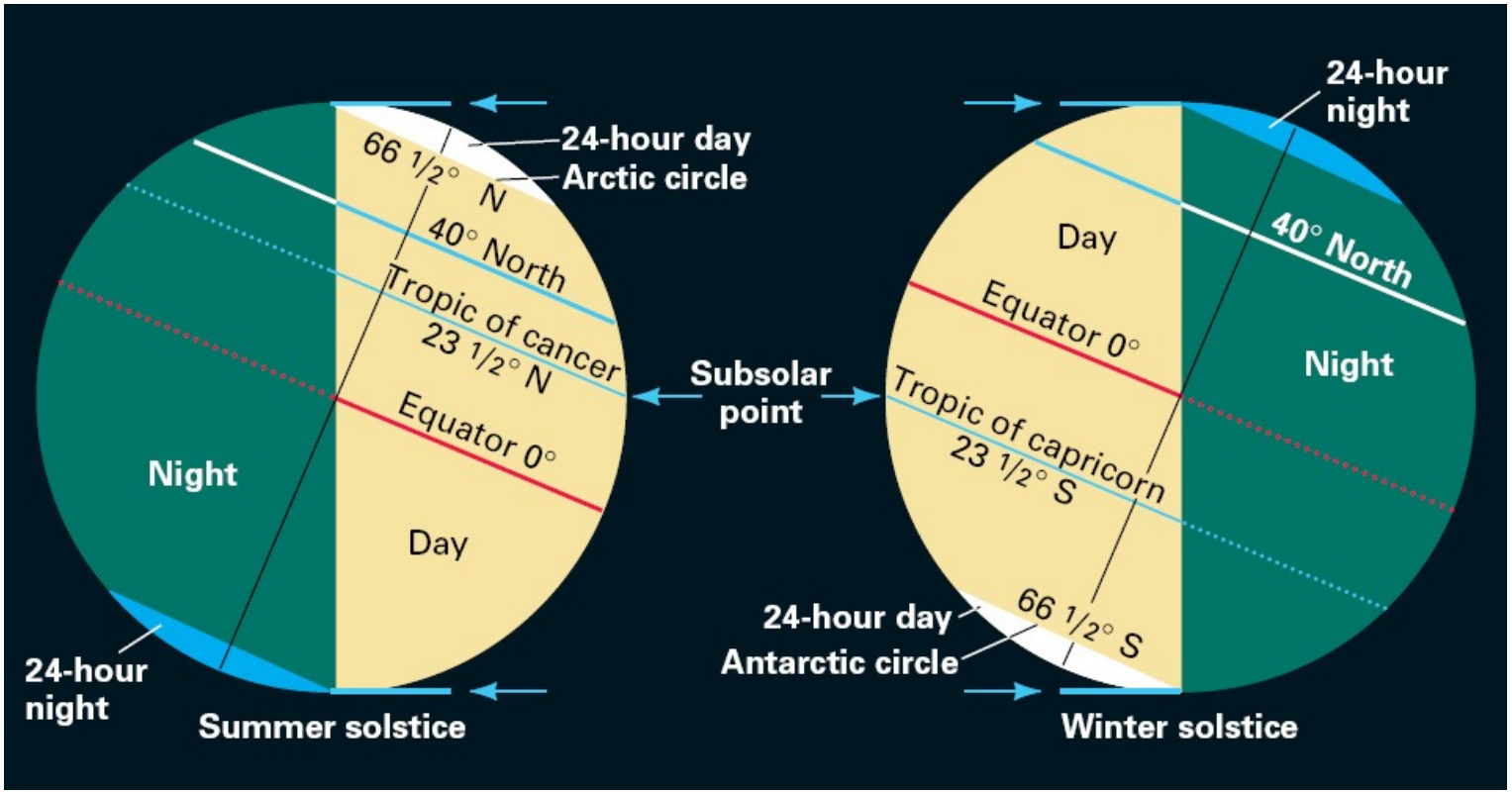

Strahler,2002

Declination over the year

the latitude of the subsolar point marks the sun's declination which changes throughout the year

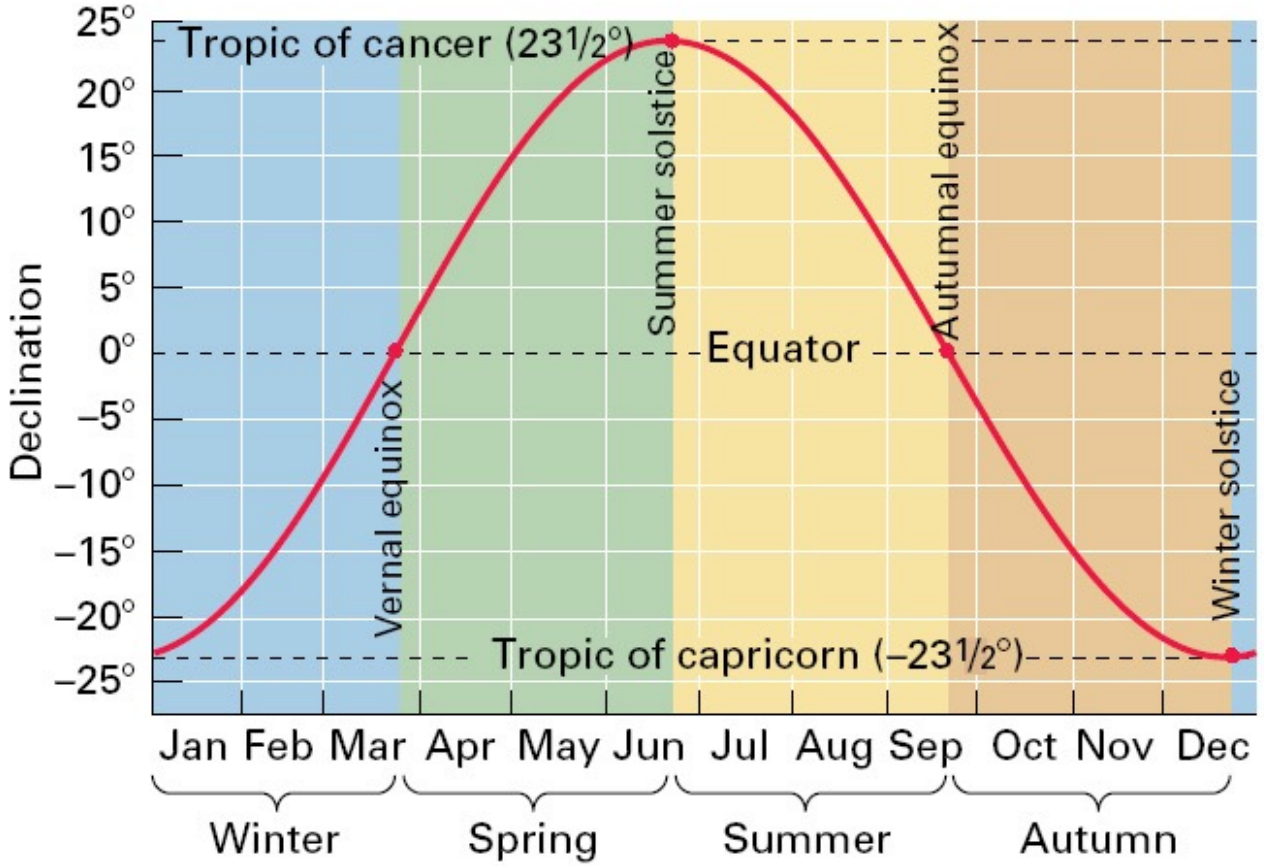

Strahler,2002

Configuration of the earth‘s orbit 9000 years ago

Today:
Perihelion in January

Tilt of the earth‘s axis:
23.5°

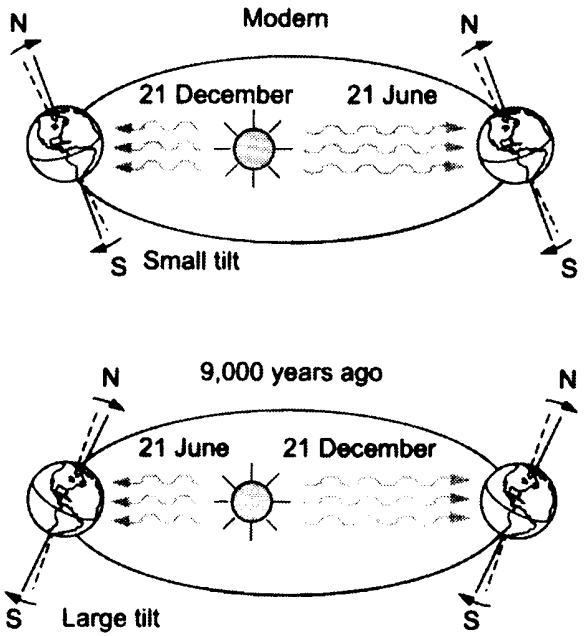

9000 years ago::
Perihelion in July

Tilt of the earth‘s axis:
24.0°

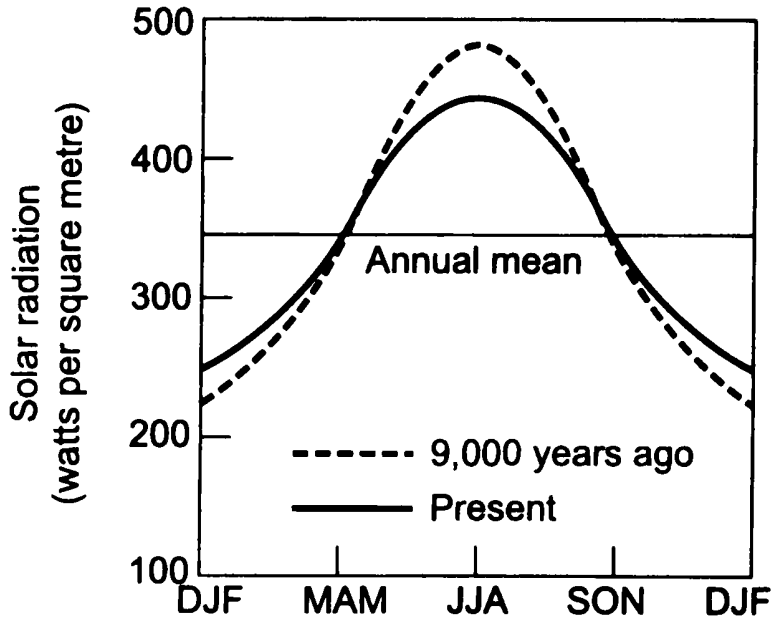

Changes in the **Earth's elliptical orbit** from the present configuration to **9,000 years ago**.(left)

Changes in the average **solar radiation during the year** over the **northern hemisphere** (right).
The incoming solar energy averaged over the northern hemisphere was ca. 7 % greater in July
and correspondingly less in January.

Kutzbach in „Climate System Modelling“ (1992). Houghton, J.: „ Global Warming“ (1997)

Orbital parameters

time

Excentricity

Periods:
100, 400 ky

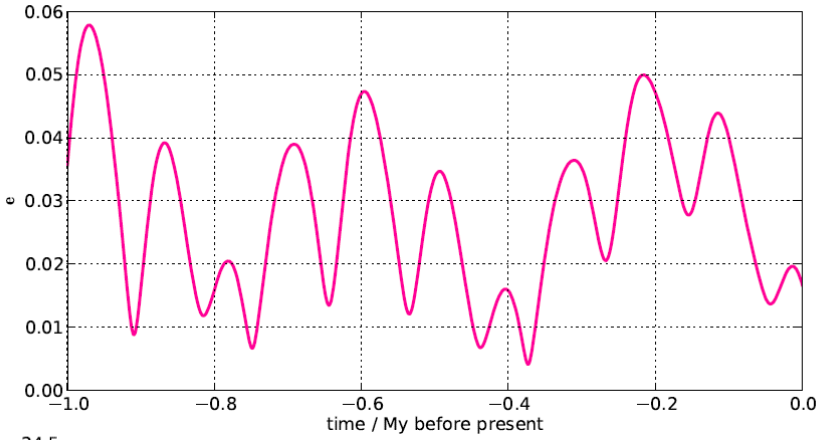

Obliquity

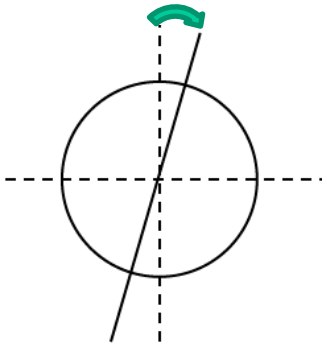

Periods:
39, 41, 54 ky
Modul. 1.2 My

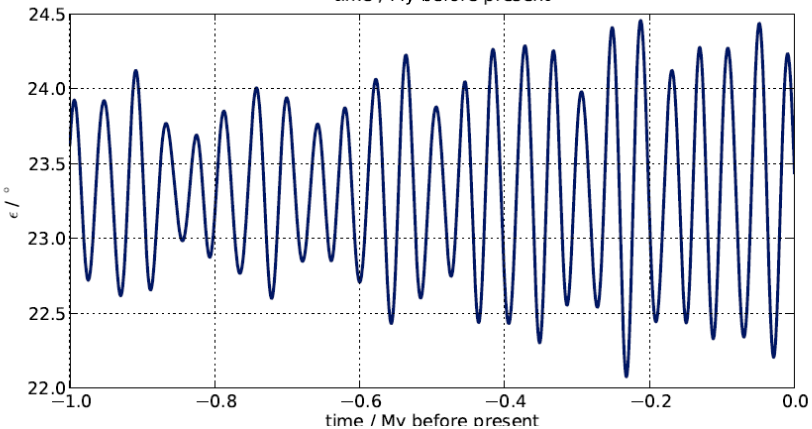

Precession

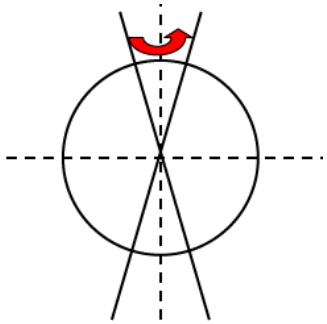

Periods:
19, 23 ky
Modul. Excentr

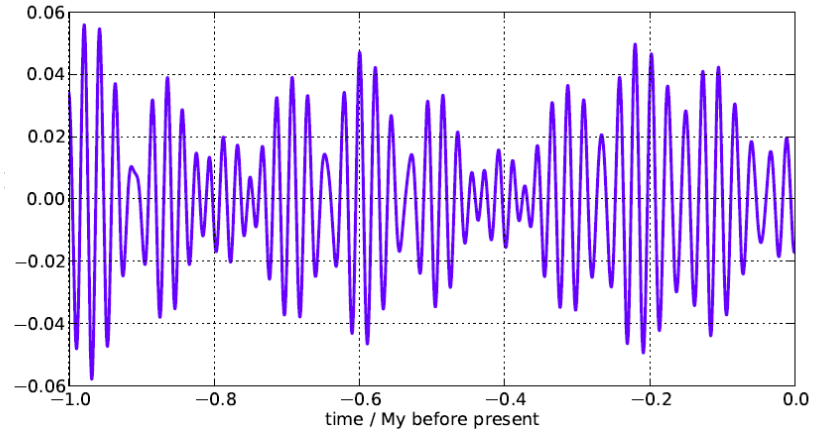

Resulting Effect

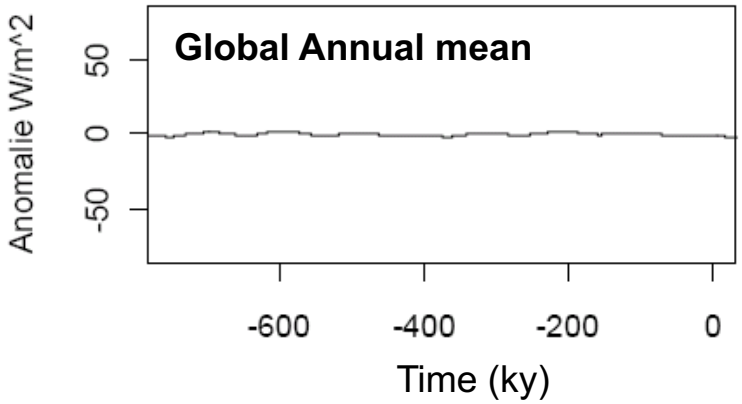

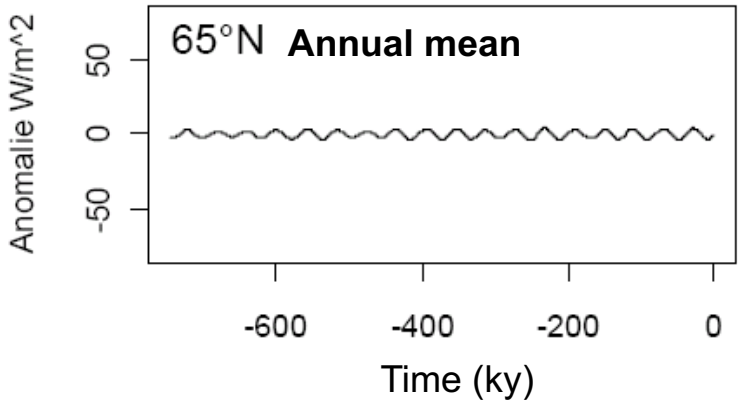

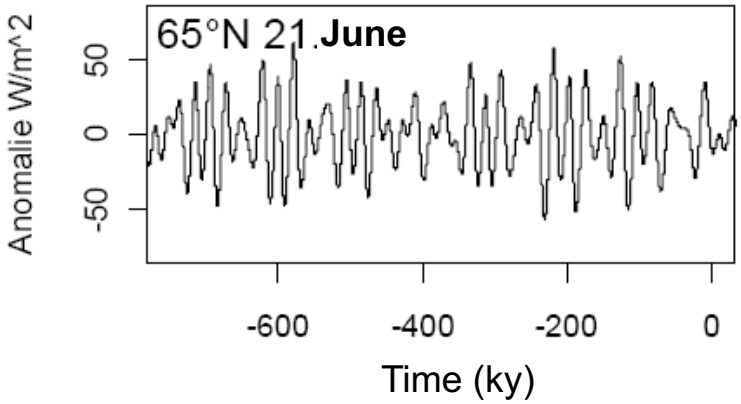

Non-linearities are important

Ansätze

- Global Concept (Imbrie 92)

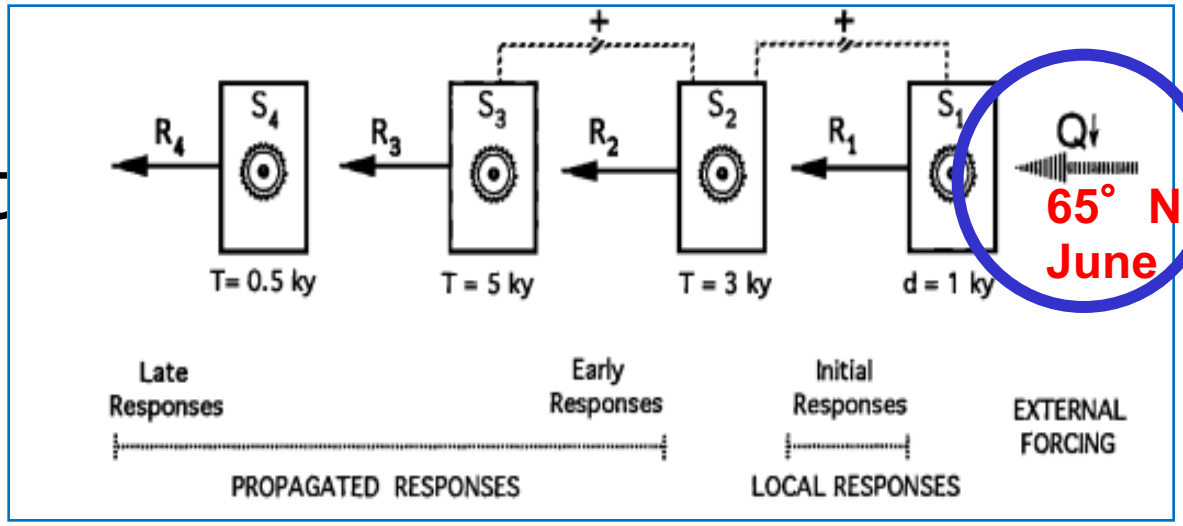

- Local Model (Short et al., 91) 2D linear EBM

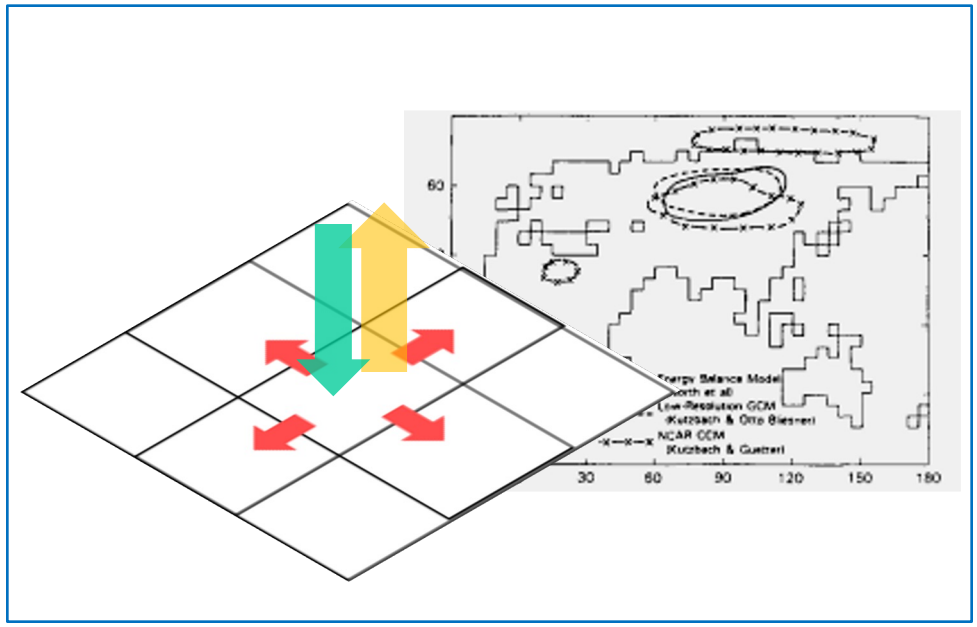

- Complex Models

  Computer

Ice ages

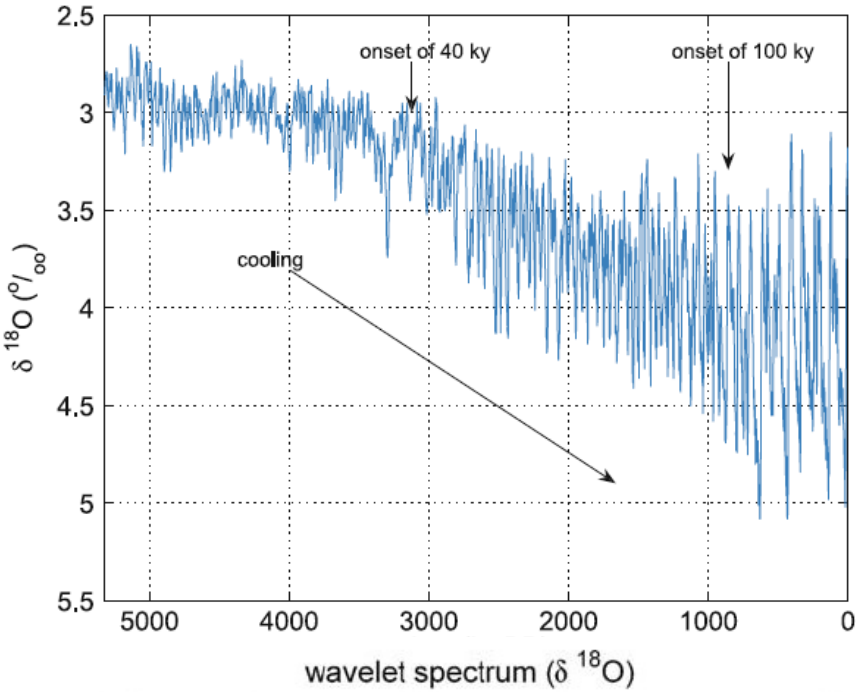

wavelet spectrum ($\delta^{18}O$)

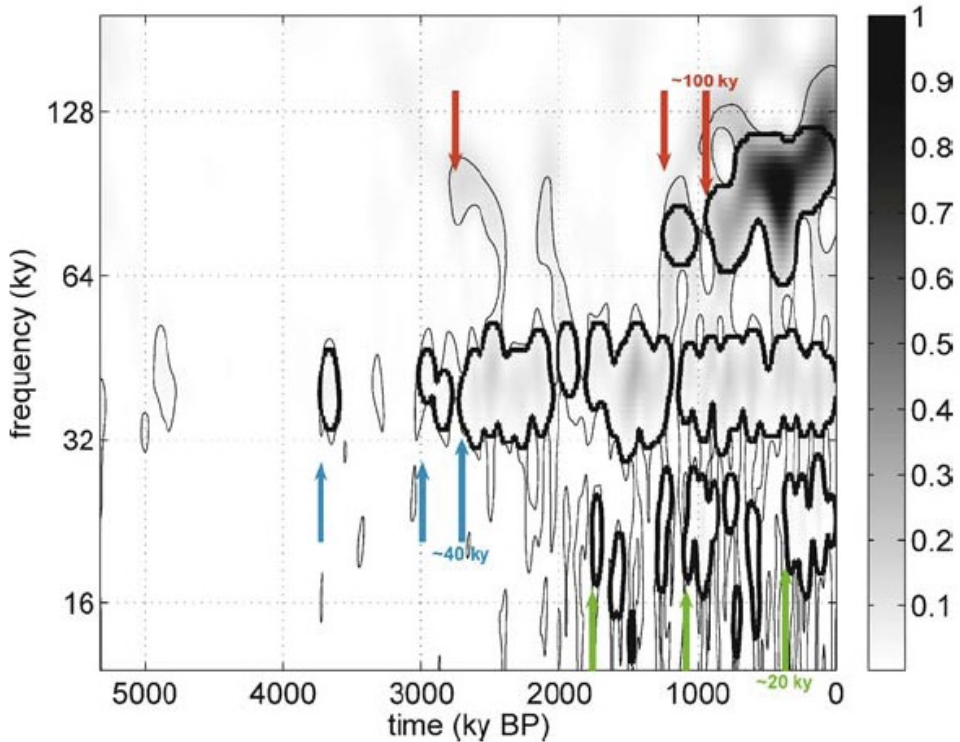

A holy grail

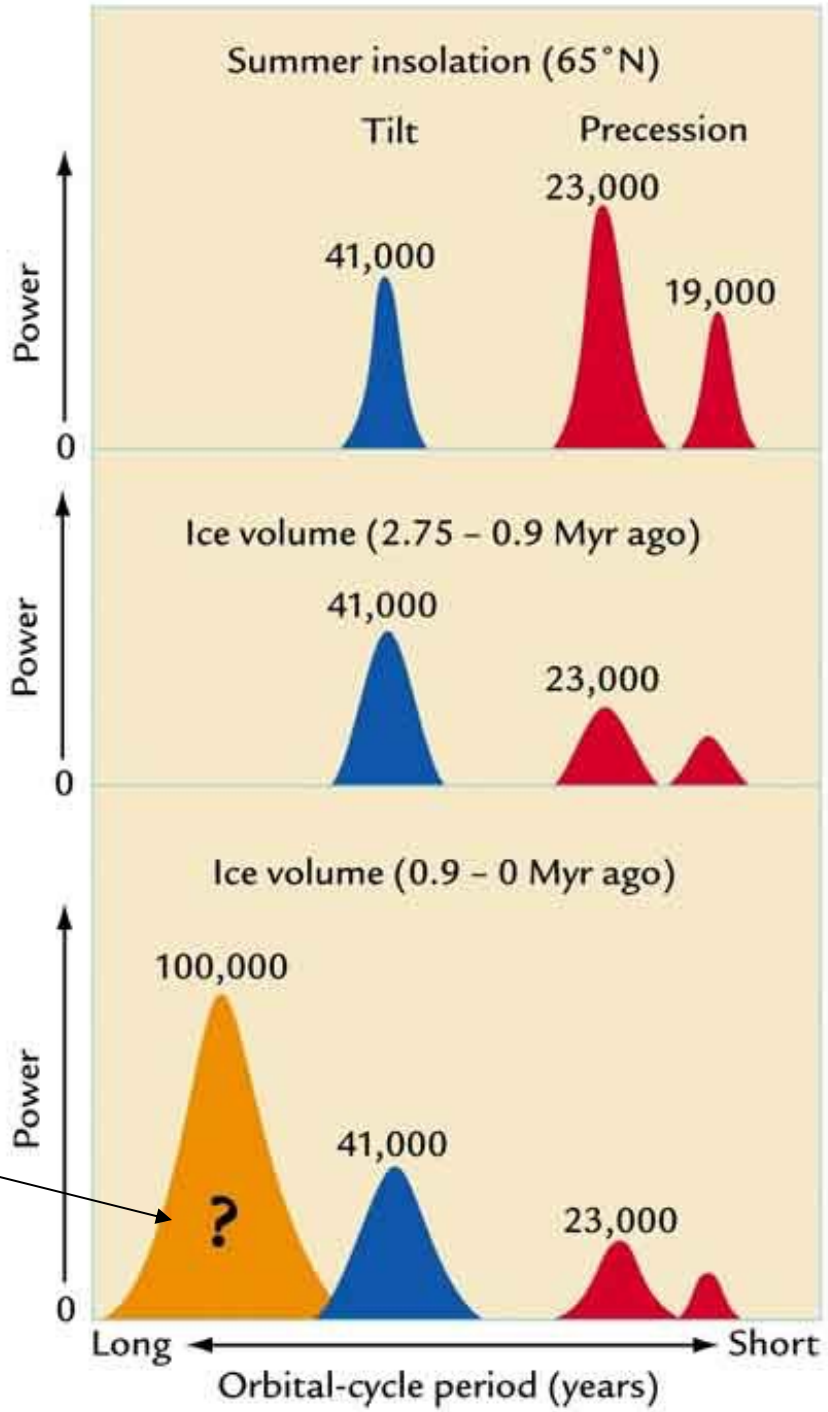
Summer insolation (65°N)
Tilt
Precession
23,000
41,000
19,000
Power
0
Ice volume (2.75 – 0.9 Myr ago)
41,000
23,000
Power
0
Ice volume (0.9 – 0 Myr ago)
100,000
41,000
23,000
?
Power
0
Long
Short
Orbital-cycle period (years)

Theory of ice ages

External:

Increased eccentricity of the earth's orbit

Changes in the intensity of solar radiation

The earth passing through cold regions of space

Internal: ice sheet, CO2, stochastic

Amplifiers: thresholds, rectification

Insolation

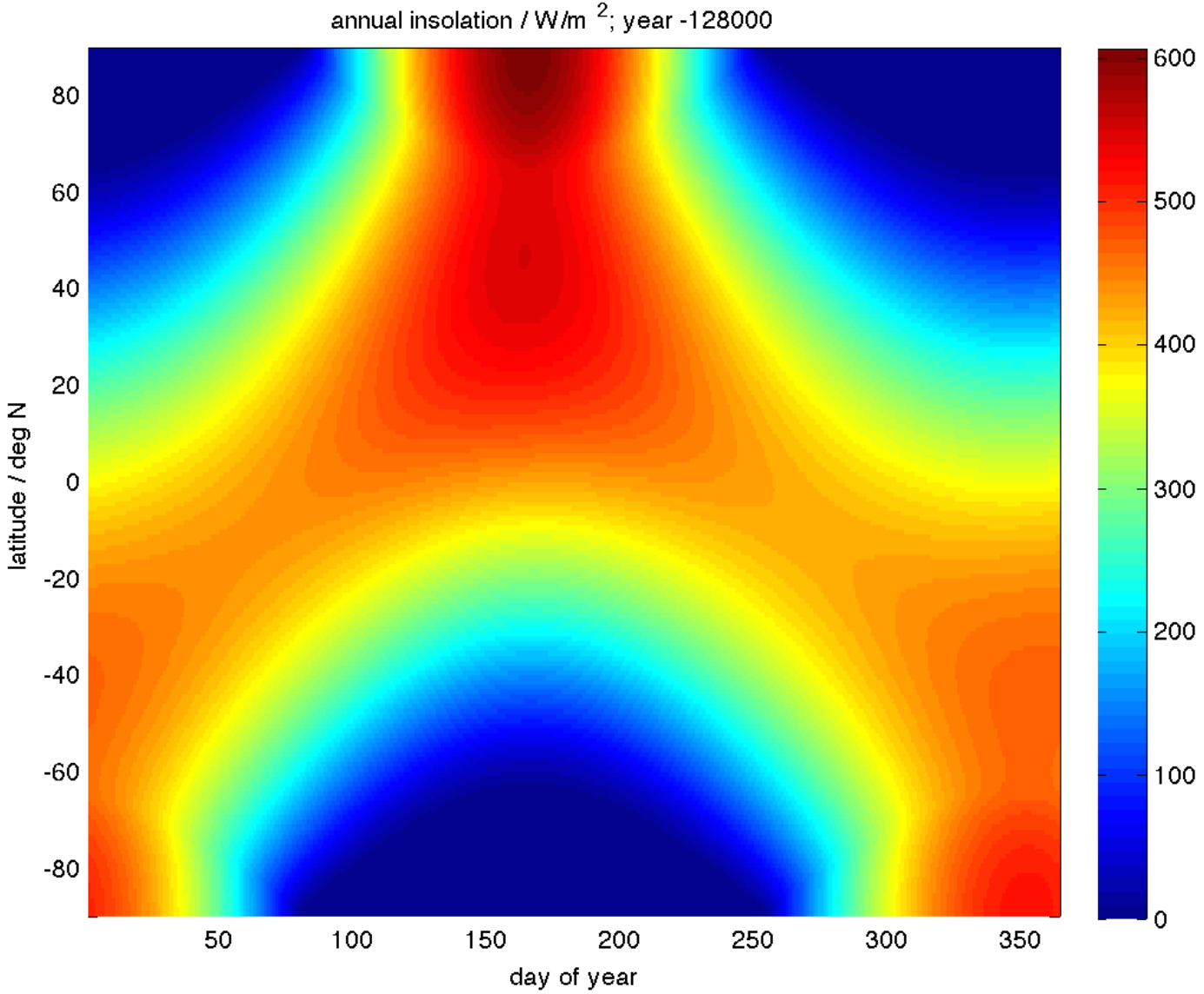
annual insolation / W/m 2; year -128000
latitude / deg N
80
60
40
20
0
-20
-40
-60
-80
50
100
150
200
250
300
350
day of year
600
500
400
300
200
100
0

Insolation anomaly

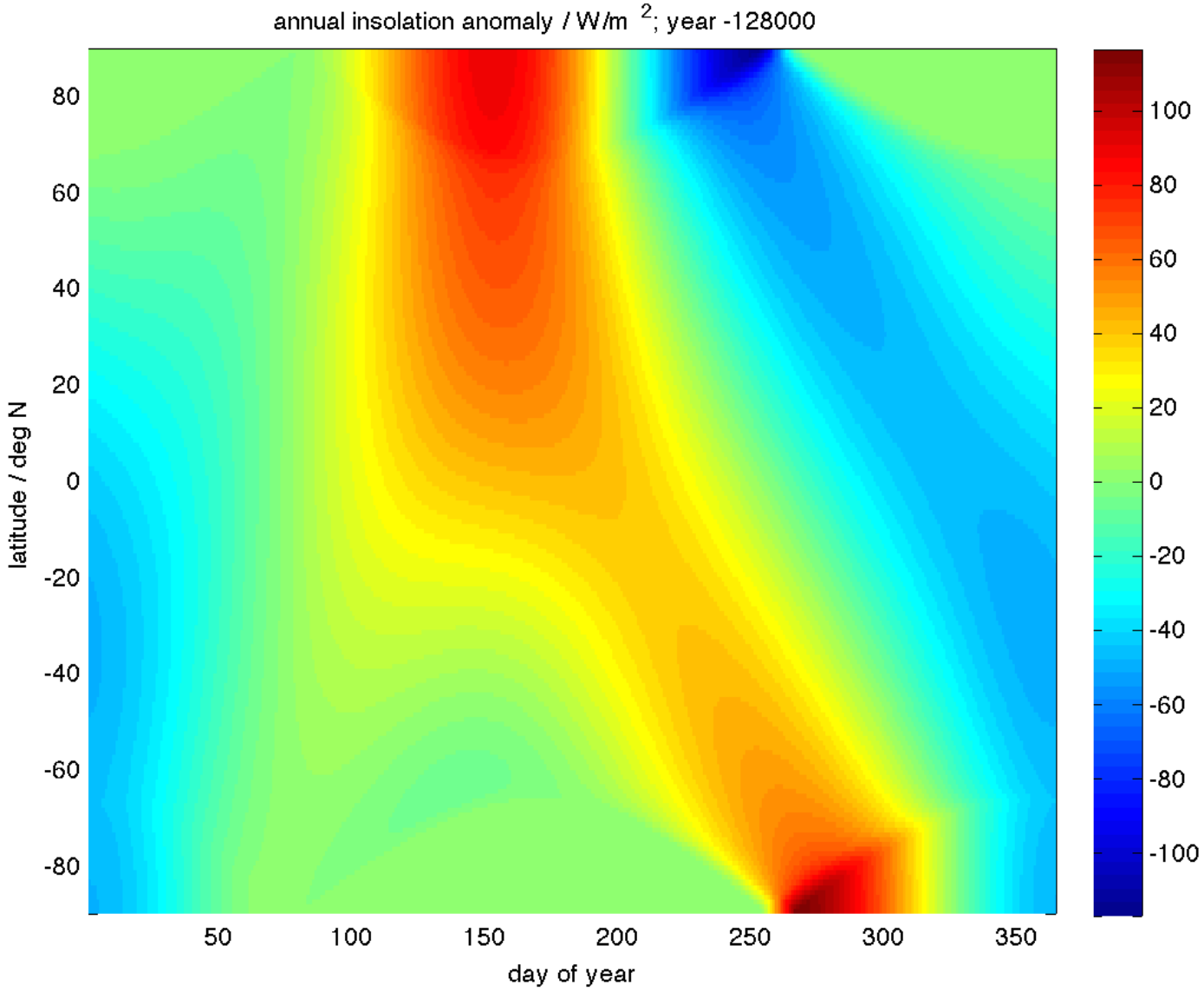

Insolation (6k minus present)

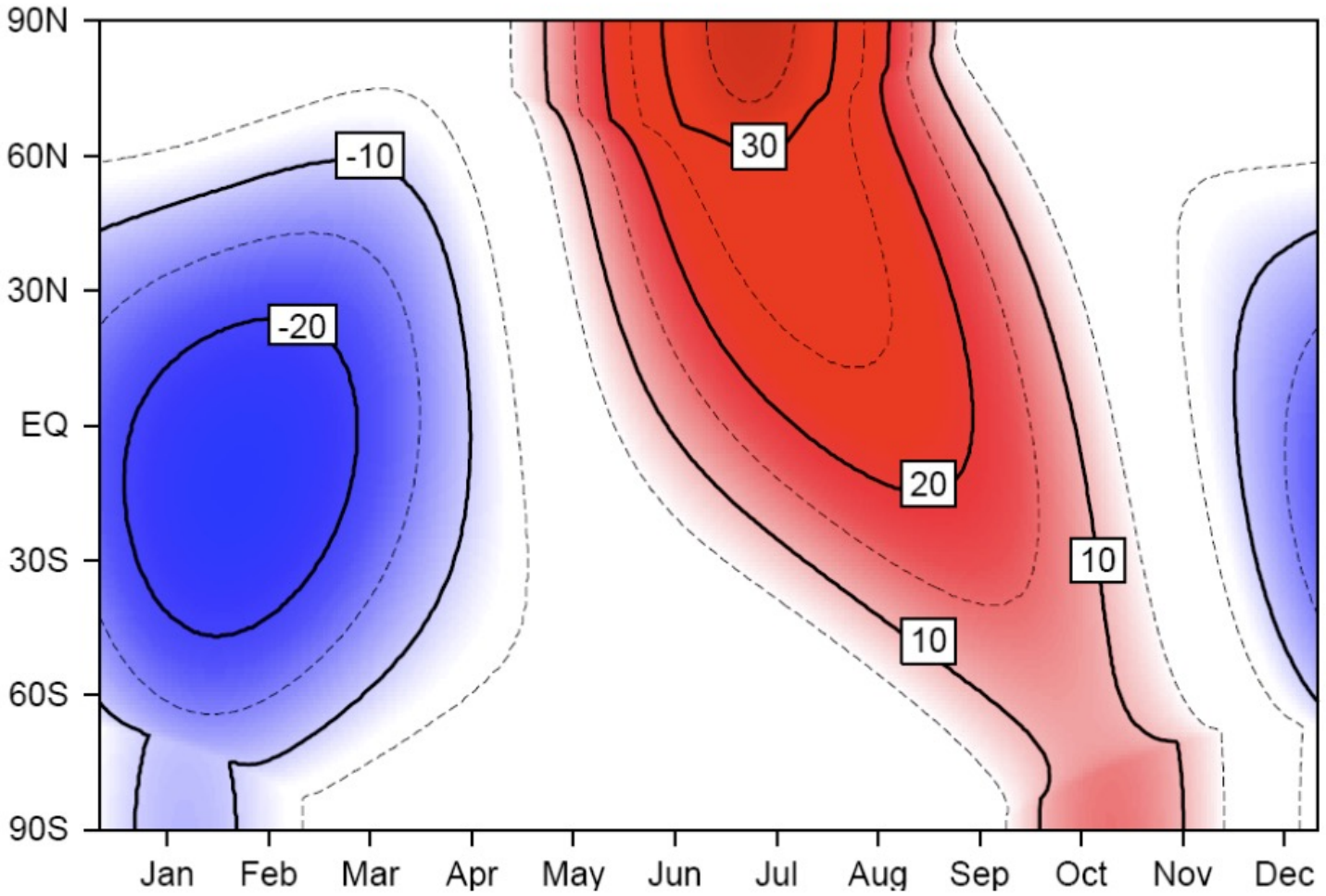

The last 120,000 years

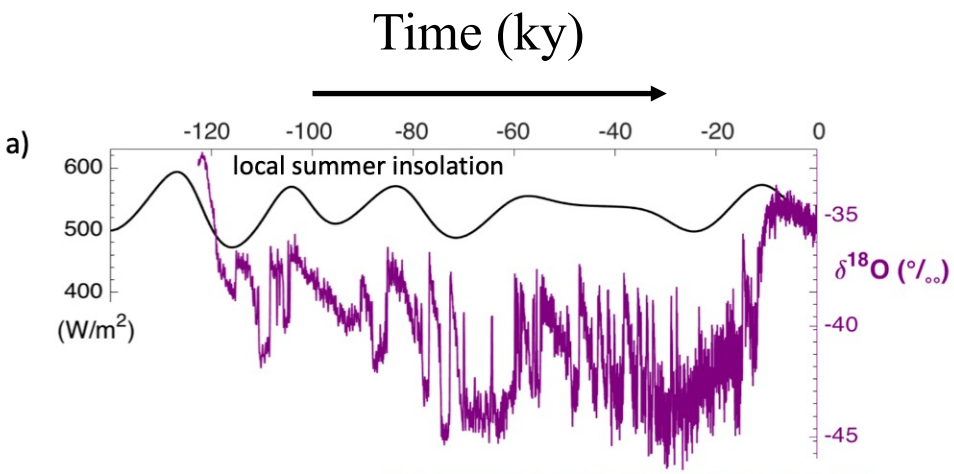

Modulation of local insolation

NGRIP, 2004; Berger, 1988

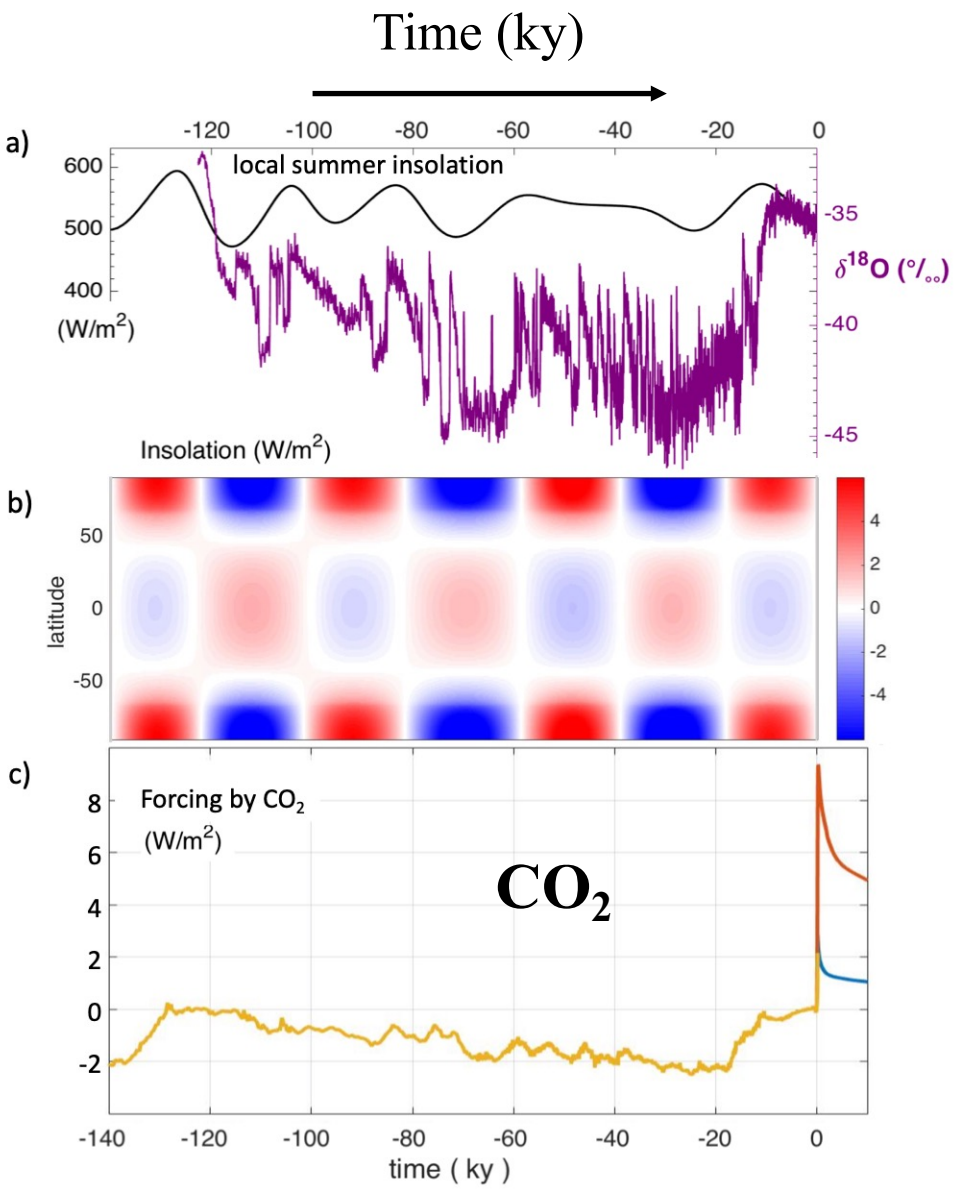

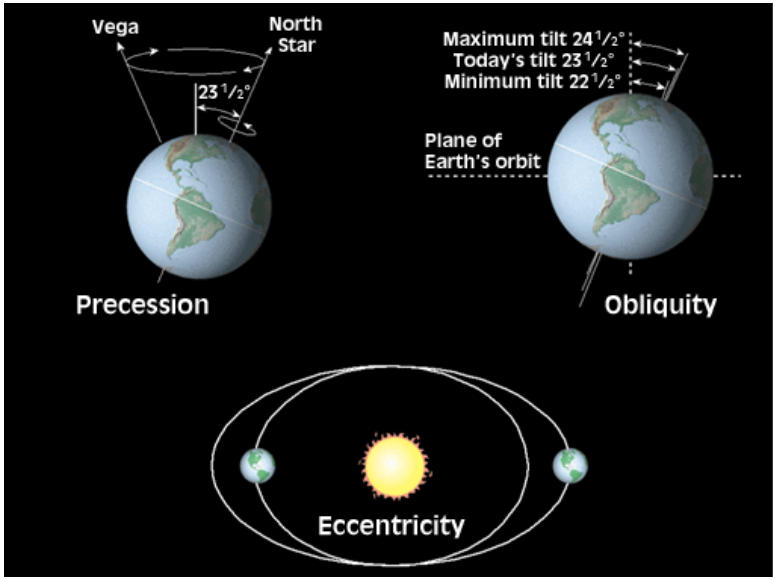

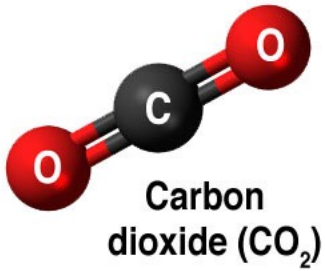

Lohmann et al. (2020) based on NGRIP, 2004; Berger, 1988; Köhler et al., 2017; Archer and Brovkin, 2008

Glacial-Interglacial variability

Global Sea Level [m]

(Bintanja et al., 2005)

CO_2 [ppmv]

From ice cores (EPICA, 2009)

Temp. anomaly "O-18" [° C]

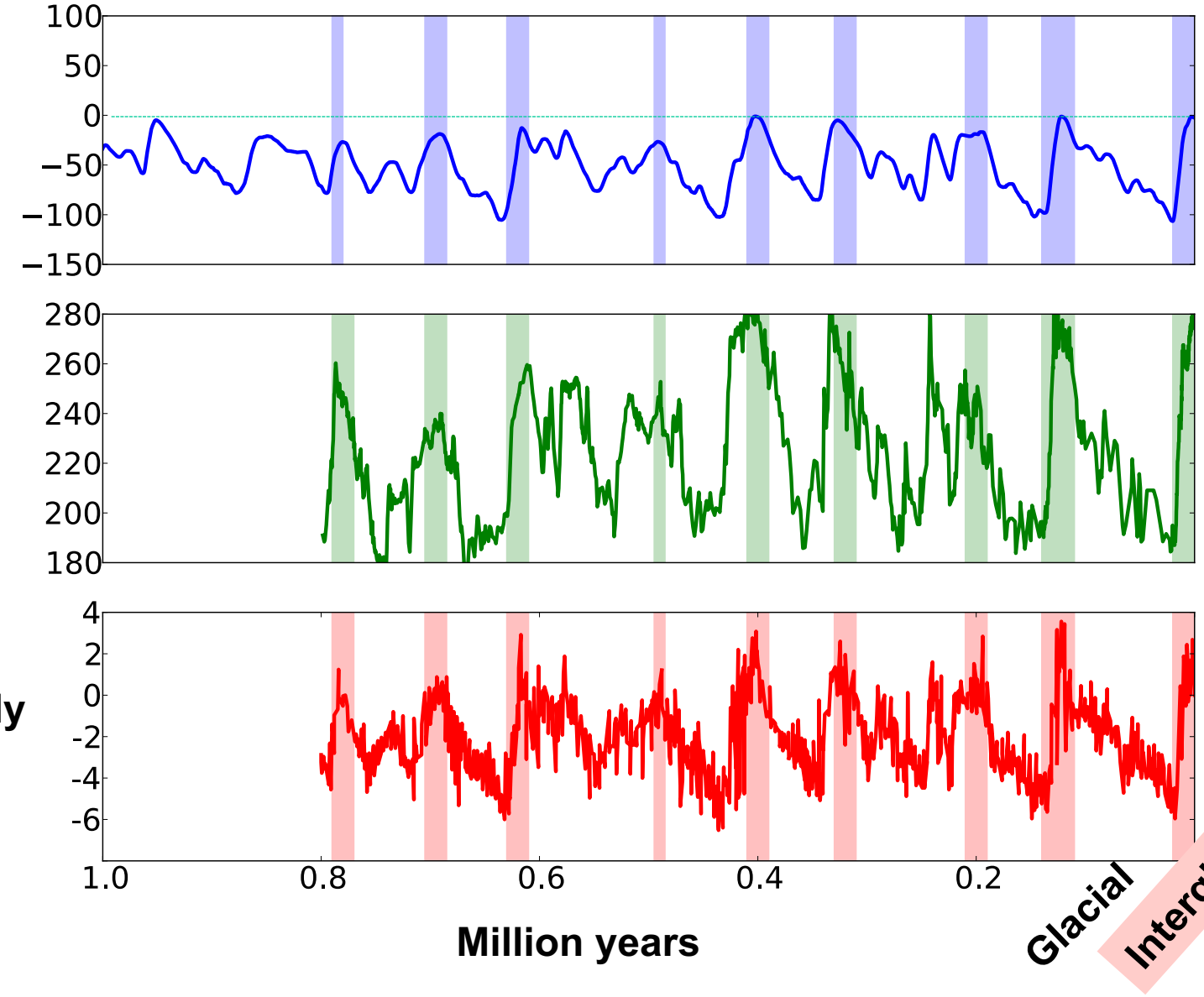

Monsoon: seasonal signal

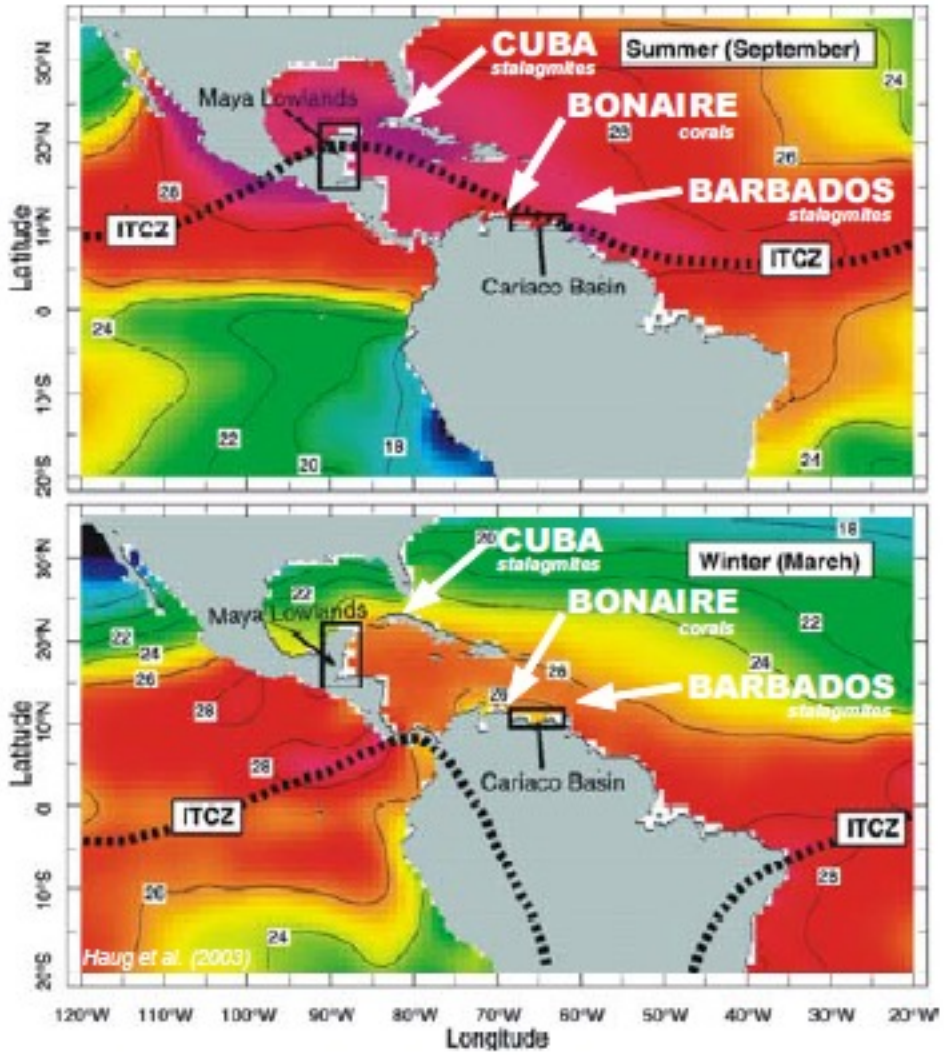

Figure 1. Seasonal variations in the mean position of the Intertropical Convergence Zone (ITCZ) over the Caribbean region, illustrated for typical summer (September) **(top)** and winter (March) **(bottom)** conditions. These variations control the pattern and timing of regional rainfall. Numbers and colours reflect sea surface temperatures in degrees Celsius. Locations of the study areas (Bonaire, Cuba, Barbados) and the Cariaco Basin and Maya Lowlands are indicated. Figure and legend modified from (Haug et al., 2003).

Monsson

seasonal reversing wind accompanied by corresponding changes in precipitation, but is now used to describe seasonal changes in atmospheric circulation and precipitation associated with the asymmetric heating of land and sea.

The English monsoon came from Portuguese monção, ultimately from Arabic mawsim (موسم "season") and/or Hindi "mausam", "perhaps partly via early modern Dutch monsun".

During warmer months sunlight heats the surfaces of both land and oceans, but land temperatures rise more quickly.
water heat capacity (4.2 J g−1 K−1)
dirt, sand, and rocks heat capacities (0.19 to 0.35 J g−1 K−1)

difference in pressure causes sea breezes to blow from the ocean to the land, bringing moist air inland

https://en.wikipedia.org/wiki/Monsoon

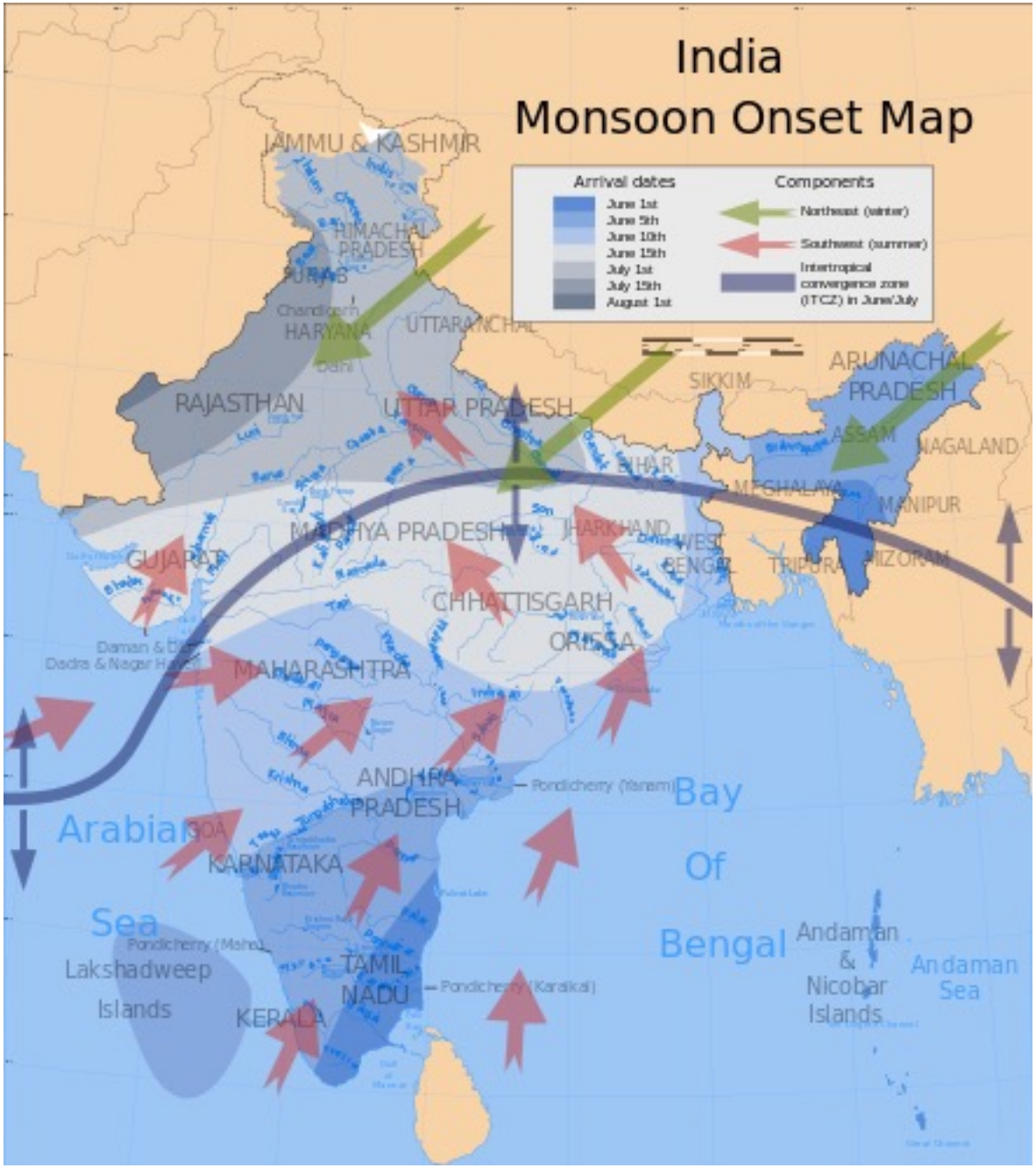
India
Monsoon Onset Map
Arrival dates
June 1st
June 5th
June 10th
June 15th
July 1st
July 15th
August 1st
Components
Northeast (winter)
Southwest (summer)
Intertropical convergence zone (ITCZ) in June/July
JAMMU & KASHMIR
HIMACHAL PRADESH
PUNJAB
Chandigarh
HARYANA
Delhi
UTTARANCHAL
RAJASTHAN
UTTAR PRADESH
SIKKIM
ARUNACHAL PRADESH
ASSAM
NAGALAND
BIHAR
MEGHALAYA
MANIPUR
MADHYA PRADESH
JHARKHAND
WEST BENGAL
TRIPURA
MIZORAM
GUJARAT
CHHATTISGARH
ORISSA
Daman & Diu
Dadra & Nagar Haveli
MAHARASHTRA
ANDHRA PRADESH
Pondicherry (Yanam)
Arabian
Sea
GOA
KARNATAKA
Bay
Of
Bengal
Andaman
&
Nicobar
Islands
Andaman
Sea
Pondicherry (Mahe)
Lakshadweep
Islands
TAMIL NADU
Pondicherry (Karaikal)
KERALA

Precession: Effect on climate

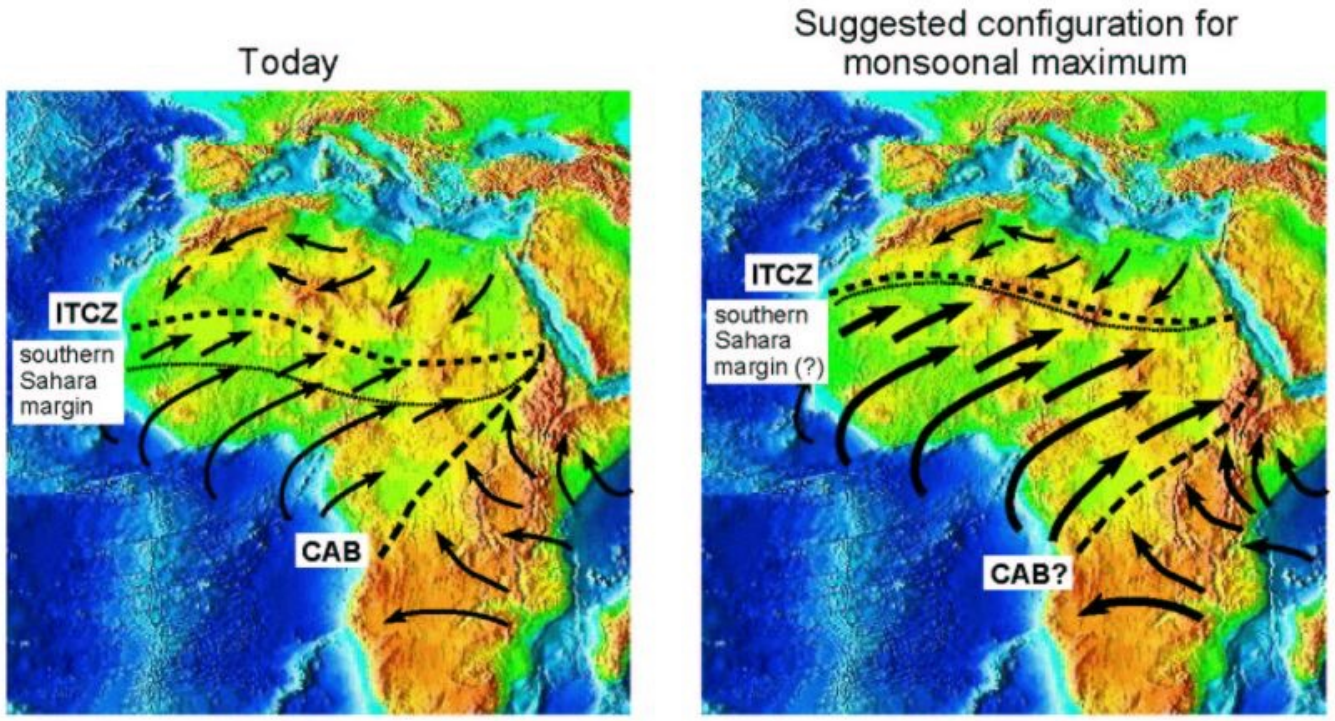

Rough locations of the Intertropical Convergence Zone (ITCZ), the Congo Air Boundary (CAB), and the southen margin of the Sahara Desert for the present-day, and for the monsoonal maximum.

Holocene 6K- PI, precipitation JJA

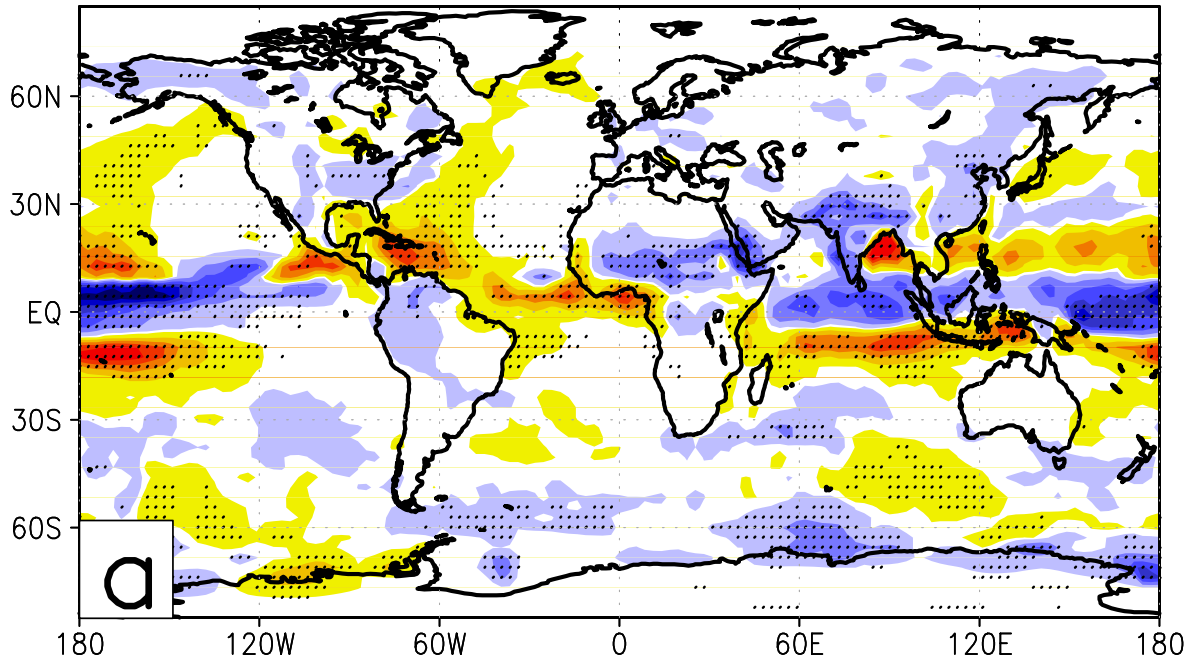

Paintings

Mestikawi-Foggini-Höhle
Foggini-Höhle
Höhle Wadi Sura II

Older than 7000 years

2002 Archäologen Massimo & Jacopo Foggini, Ahmed Mestikawi

Agadez in Niger.

Sahel Zone

The famine in the Sahel in the 1970s and 1980s was the result of drought, affected about 50 million people and led to the death of an estimated one million people.

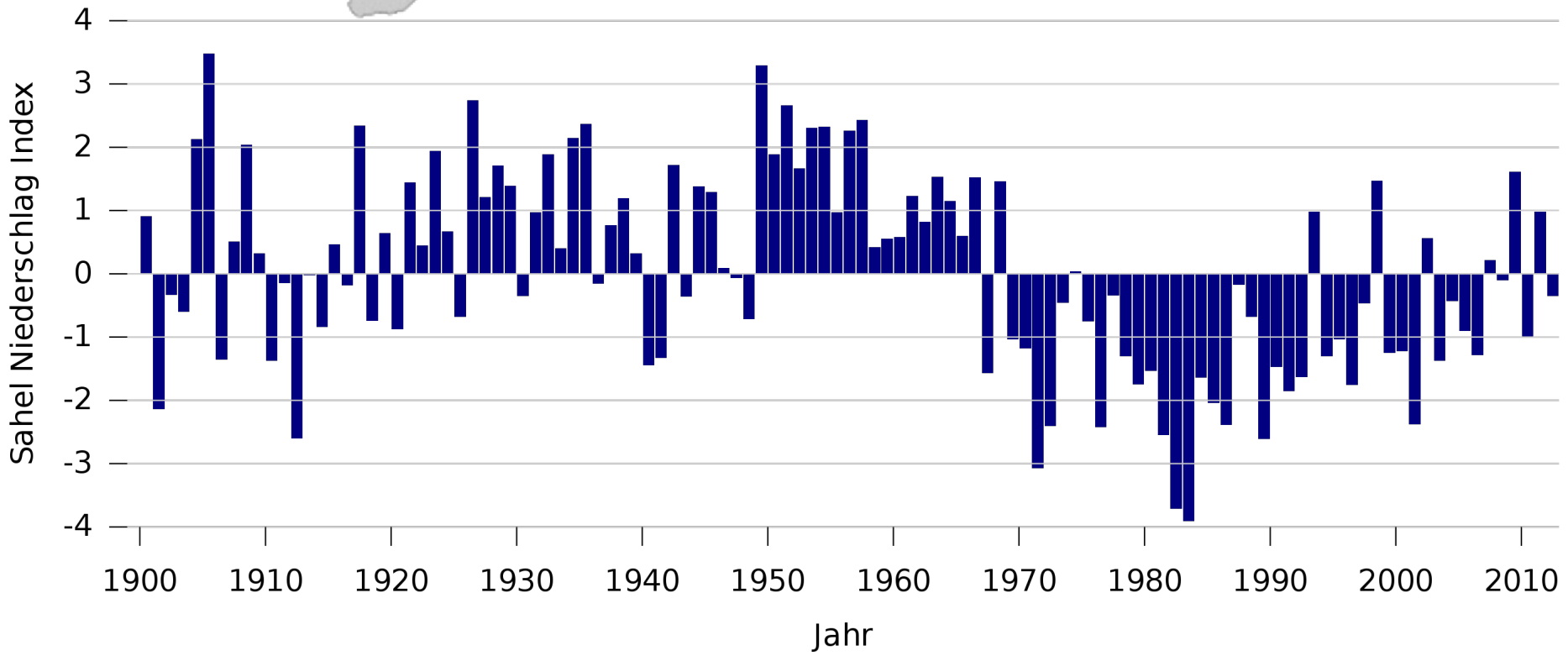

Sahel continued

- **Human impacts include deforestation, overgrazing and overexploitation of agricultural land**
- **This exacerbated the problem of desertification**
- **Another reason for the famines in the Sahel zone is that more and more locusts are invading the zone in swarms and grazing the fields**

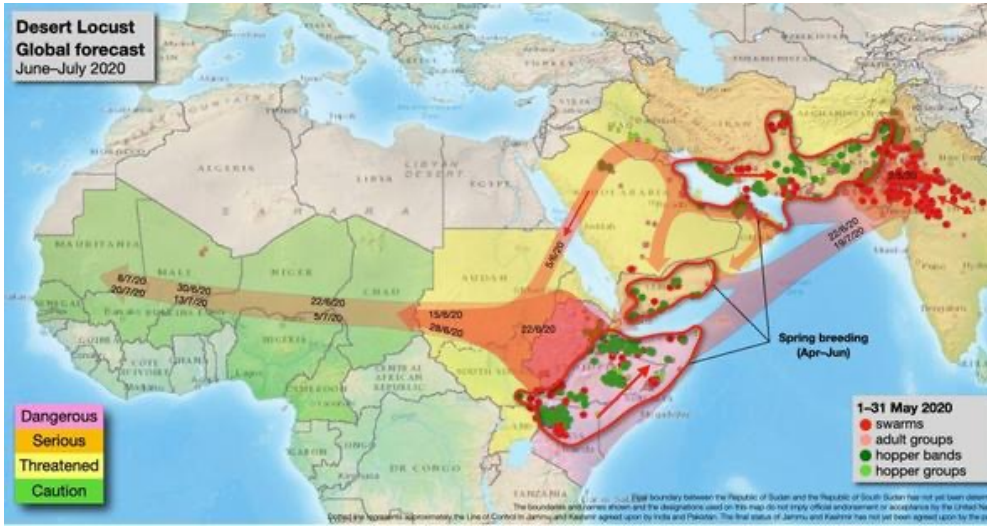

$\delta^{18}O$ Signal in the Hydrological Cycle

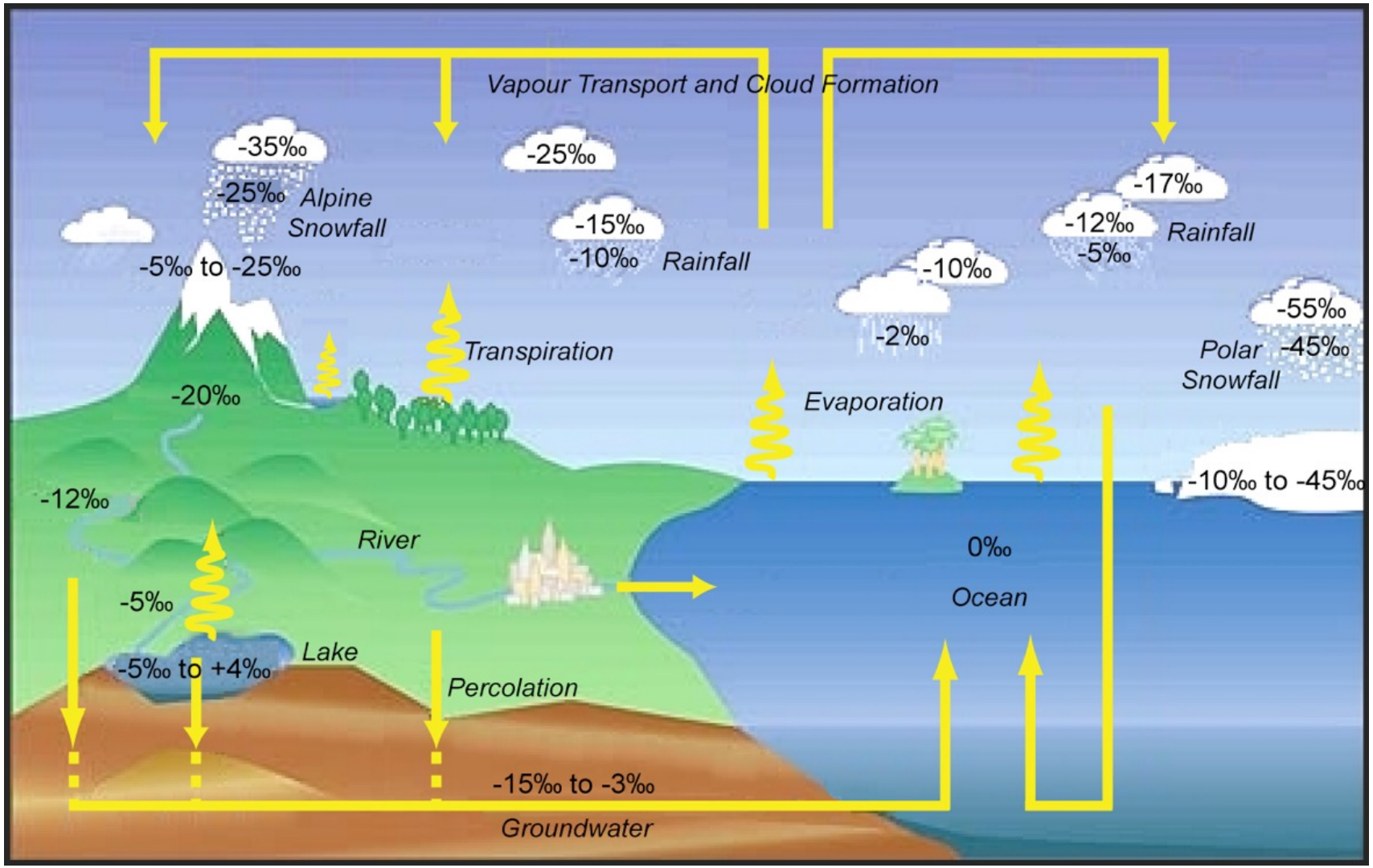

[plot adapted from the GNIP brochure, IAEA, 1996]

Scheme of typical isotope depletion in various parts of the hydrological cycle

Every phase change of a water mass is imprinted in its isotopic signature

Eemian $\delta^{18}O$ & δD

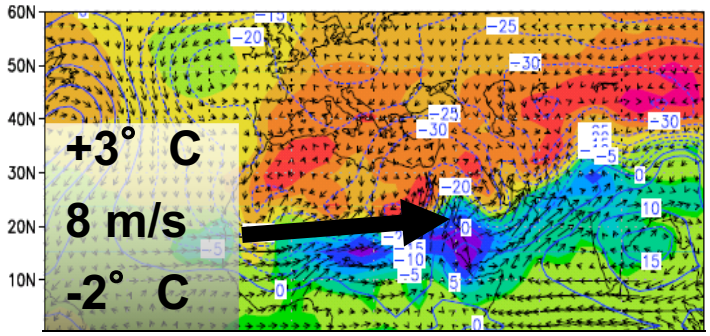

Temperature & wind

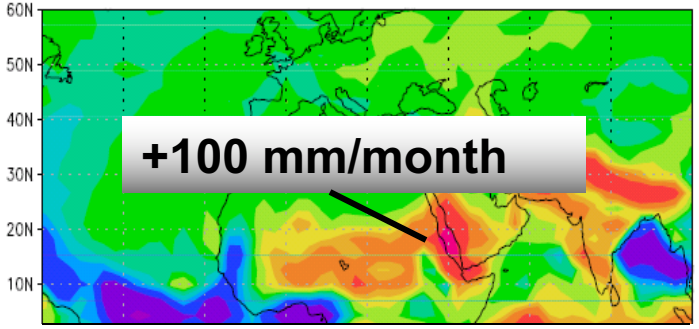

Precipitation

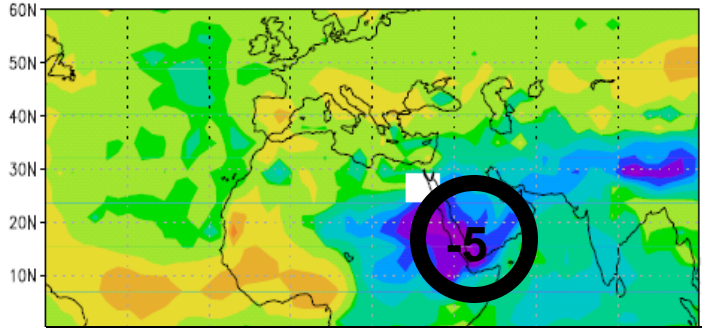

$\delta^{18}O$ (° /oo)

Using ECHAMiso

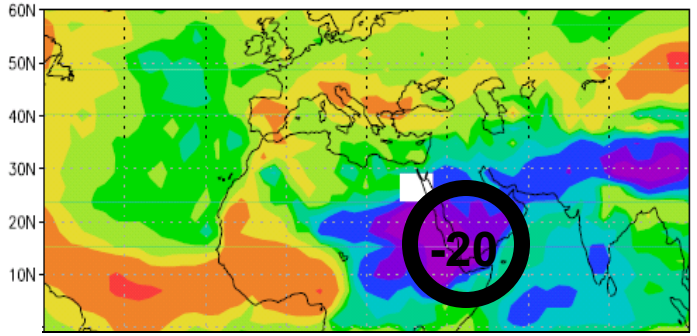

δD (° /oo)

Enhanced zonal wind & more precipitation

Isotopic Depletion: Consistent with stalagmite data

Herold and Lohmann 2009

Comparison with O isotope records: Hoti Cave

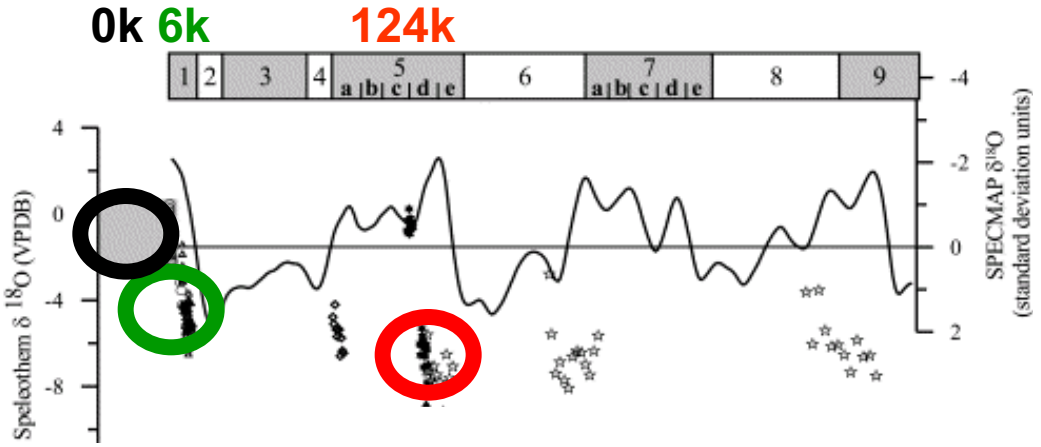

$\delta^{18}O$ (° /oo) of Speleothem

$\delta^{18}O$ (° /oo) of Precipitation

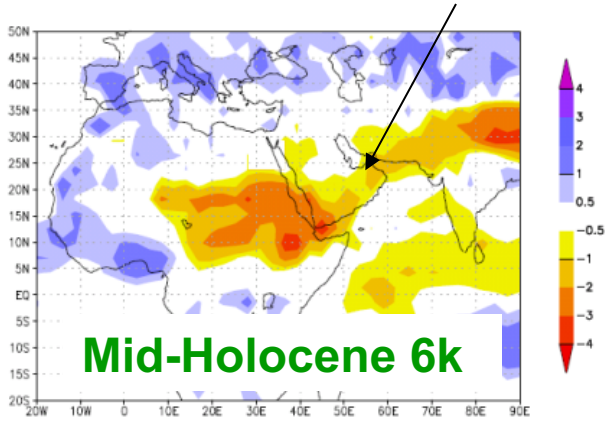

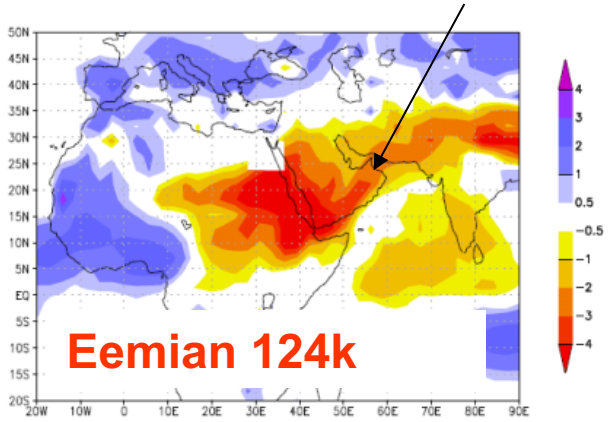

Fleitmann et al., 2003

Lohmann, Herold, Fleitmann, in prep

The use of of $\delta^{18}O$ in precipitation as a temperature proxy

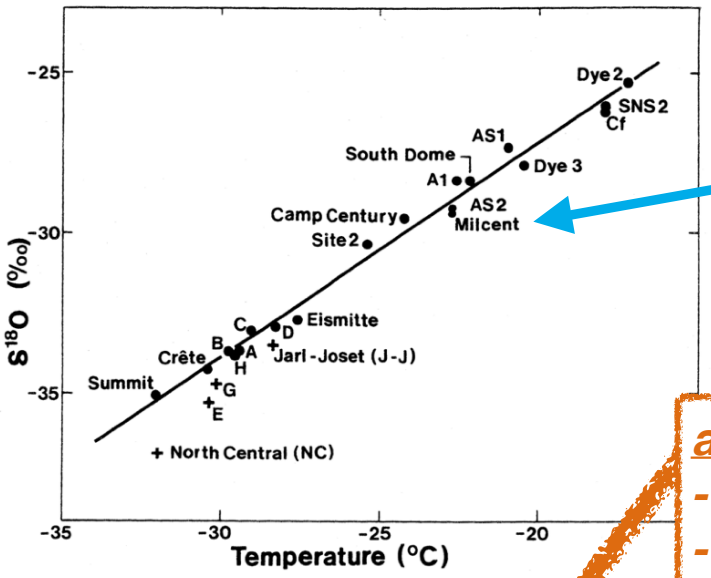

[Johnsen et al., Tellus, 1989]

Modern spatial relation between $\delta^{18}O$ and surface temperature (on Greenland):

$$\delta^{18}O = 0.67 \cdot T_{surf}$$

a priori assumption:

- temporal and spatial slopes are equal

- „constant characteristics“ of circulation processes

Converting temporal changes of $\delta^{18}O$ into past temperature changes

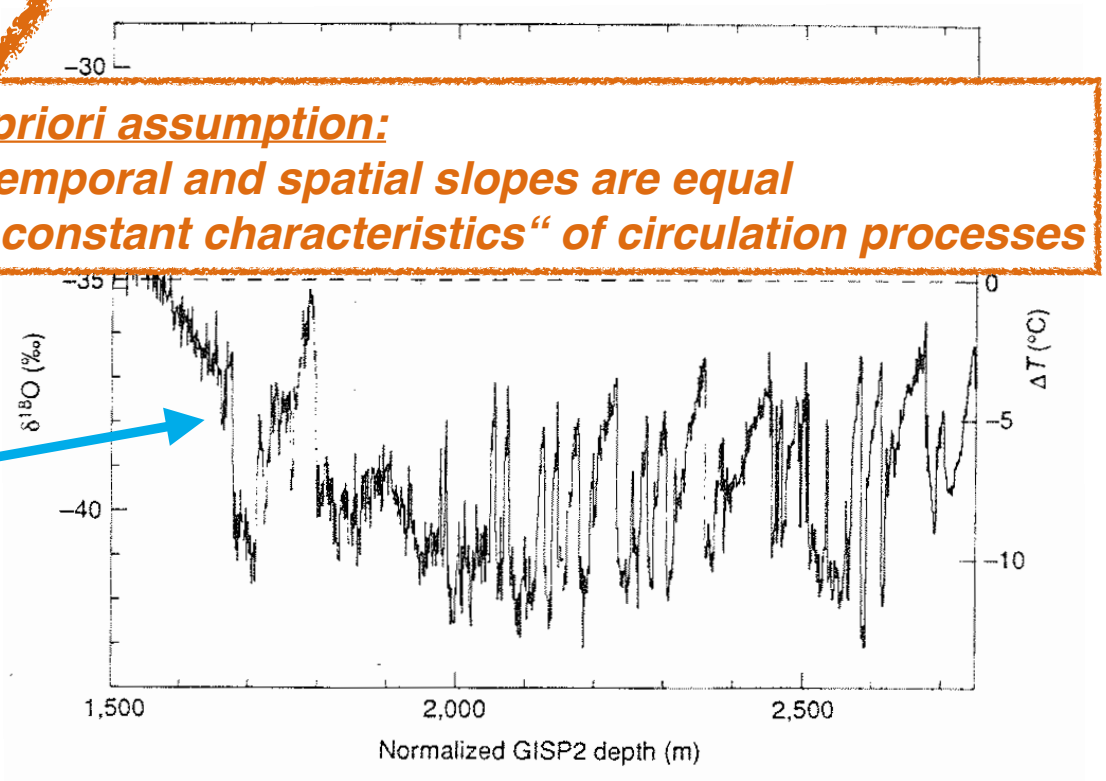

[Grootes et al., Nature, 1993]

The $\delta^{18}O$ signal in marine sediment cores

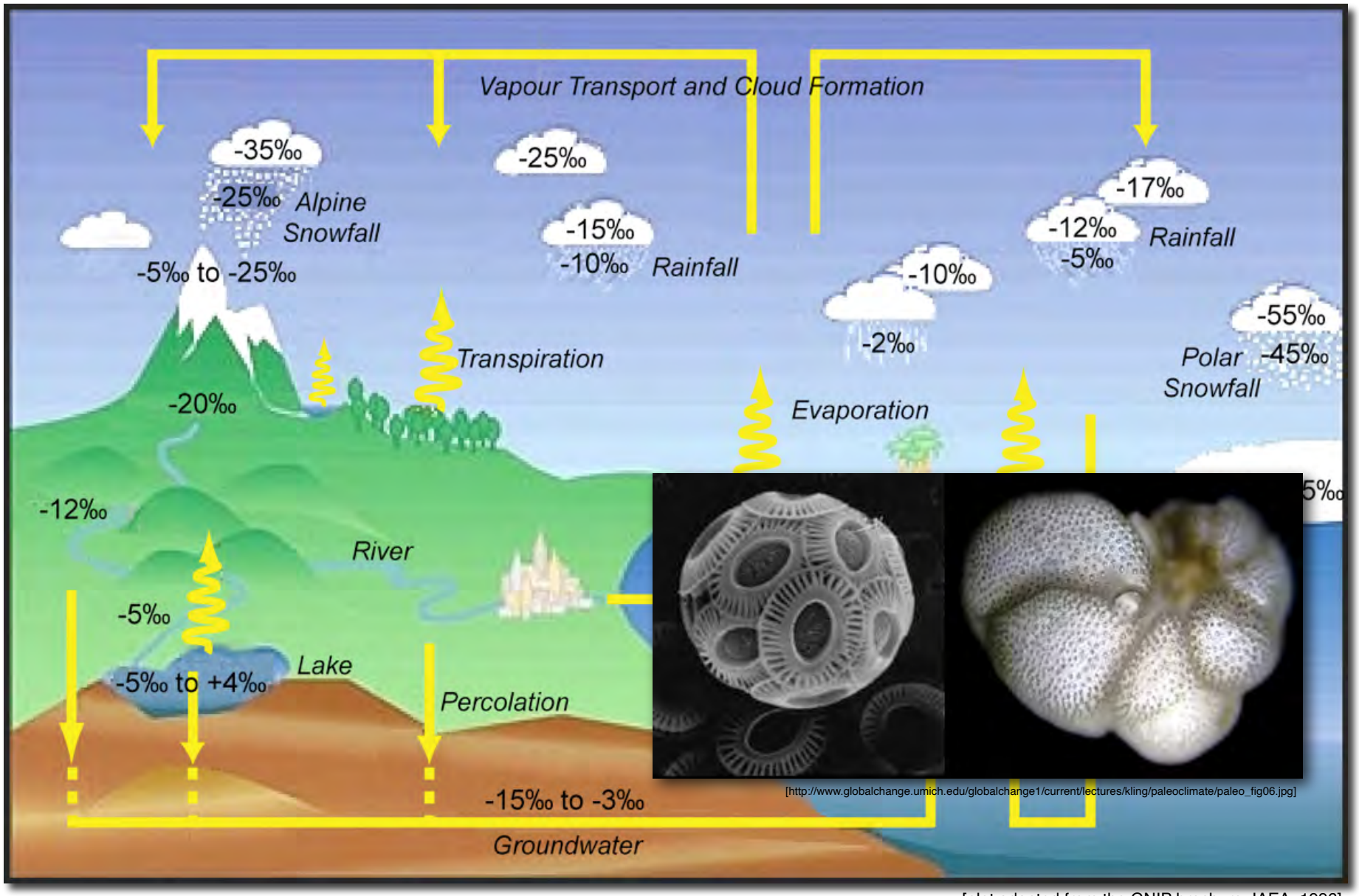

[http://www.globalchange.umich.edu/globalchange1/current/lectures/kling/paleoclimate/paleo_fig06.jpg]

[plot adapted from the GNIP brochure, IAEA, 1996]

Transformation of snow to ice

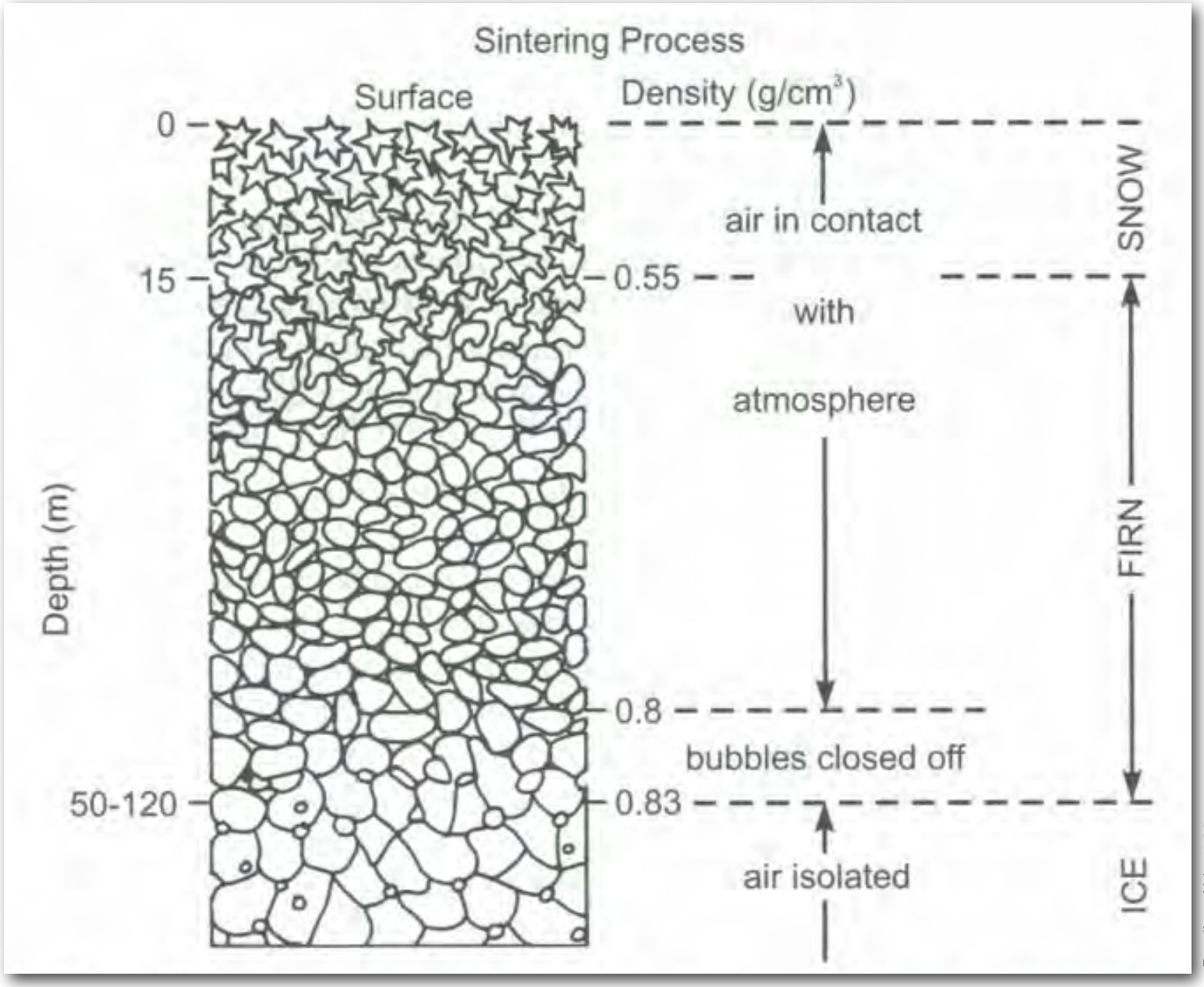

Bradley, Abb. 5.30

Example: difference between ice age and gas age

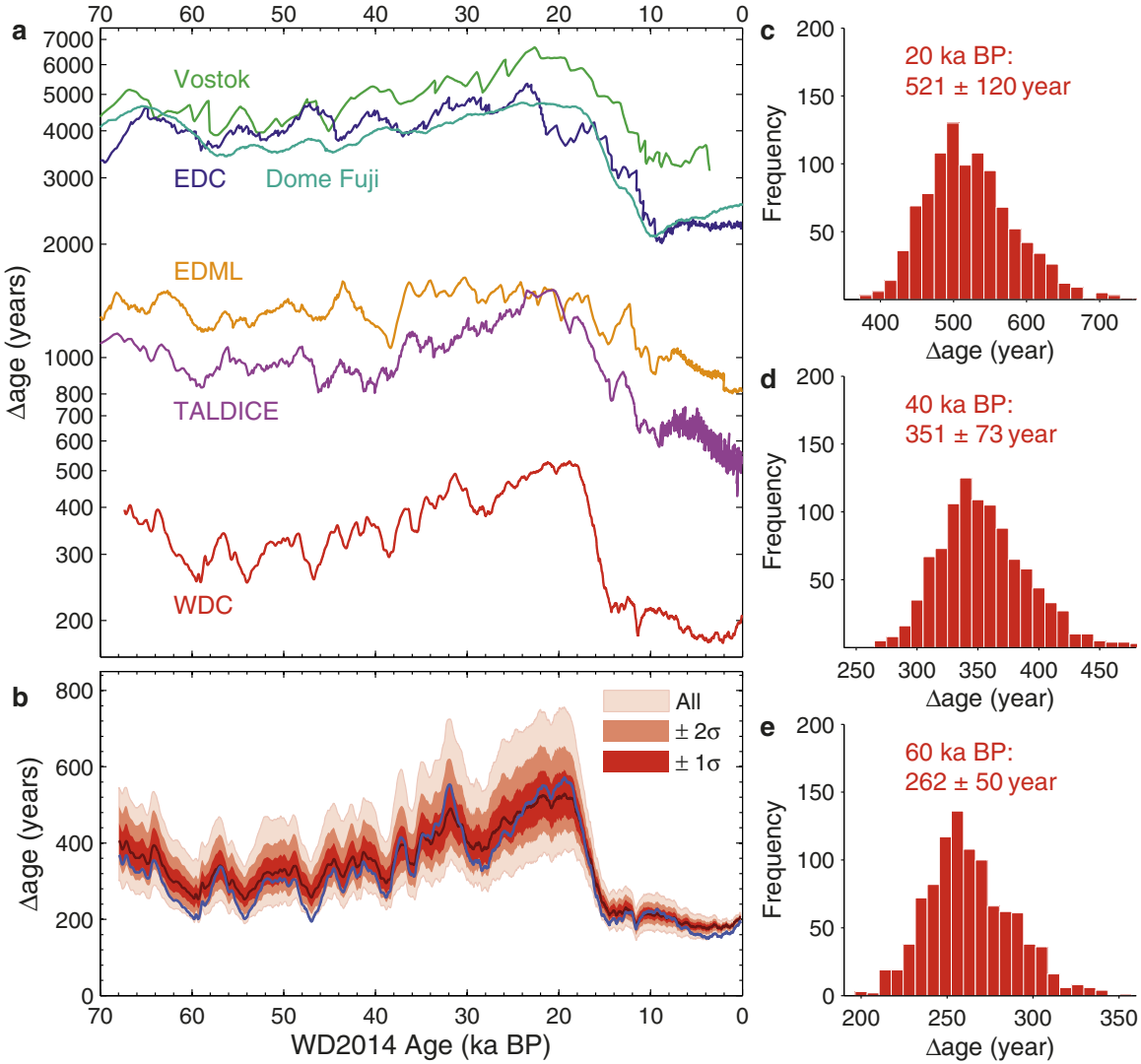

Extended Data Figure 1 | Difference between gas age and ice age (Δage) at WAIS Divide. a, Comparison of WDC Δage with other Antarctic cores. Ice core abbreviations: EDC, EPICA Dome Concordia; EDML, EPICA Dronning Maud Land; TALDICE, Talos Dome; WDC, WAIS Divide. Δage values are taken from refs 23, 63–65. The vertical axis is on a logarithmic scale. **b**, Δage uncertainty bounds obtained from an ensemble of 1,000 alternative Δage scenarios; details are given elsewhere[23]. A Δage scenario obtained with an alternative densification model (ref. 39 instead of ref. 38) is shown in blue. **c–e**, Histograms of the 1,000 Δage scenarios at 20 kyr BP (**c**), 40 kyr BP (**d**) and 60 kyr BP (**e**); stated values give the distribution mean ± the 2σ standard deviation.

WAIS Divide Project Members, Nature, 2015

Exercise

- https://paleodyn.uni-bremen.de/study/ClimII_2022_Ex1.pdf
- R markdown

http://paleodyn.uni-bremen.de/gl/tmp/Orbital.html

- Website to the Notebook including the data are at [https://www.awi.de/fileadmin/user_upload/AWI/Forschung/Klimawissenschaft/Dynamik_des_Palaeoklimas/OrbitalTheoryOfIceAges/index.html
- and here: https://www.awi.de/forschung/klimawissenschaften/dynamik-des-palaeoklimas/lehre.html